Gravitational waves from the first order electroweak phase transition in the Z_3 symmetric singlet scalar model

Toshinori Matsui [KIAS]

Collaborators:

Katsuya Hashino[1,2], Mitsuru Kakizaki[1], Shinya Kanemura[2], Zhaofeng Kang[3], Pyungwon Ko[4]

[1]U. of Toyama, [2]Osaka U., [3]Huazhong University of Science and Technology, [4]KIAS,

arXiv:1509.08394 [PRD], M. Kakizaki, S. Kanemura, TM

arXiv:1609.00297 [PLB], K. Hashino, M. Kakizaki, S. Kanemura, P. Ko, TM

arXiv:1706.09721, Z. Kang, P. Ko, TM

Electroweak symmetry breaking

- The Standard Model (SM) of the particle physics
  - Mass generation mechanism is confirmed by the discovery of the Higgs boson (*h*).
  - The SM as a low-energy effective theory is established.

$$\begin{aligned}\mathcal{L}_{\rm SM} =& \boxed{-\frac{1}{4}\left(G^{\mu\nu}\cdot G_{\mu\nu} + W^{\mu\nu}\cdot W_{\mu\nu} + B^{\mu\nu}B_{\mu\nu}\right) + \bar{\psi} i \not{\partial}\psi - \left(g_1\bar{\psi}\not{B}\psi + g_2\bar{\psi}\not{W}\psi + g_3\bar{\psi}\not{G}\psi\right)} \\ & + \boxed{|D_\mu\Phi|^2 - V(\Phi) - \bar{\psi}_i y_{ij}\psi_j\Phi + \mathrm{h.c.}}\end{aligned}$$

$$m_h = 125\ \mathrm{GeV}$$

- We have not understood the structure of the Higgs sector.
  - The SM has minimal Higgs potential. $\boxed{V_{\rm SM}(\Phi) = \mu^2|\Phi|^2 + \frac{\lambda}{2}|\Phi|^4}$ $\quad \Phi = \begin{pmatrix} w^+ \\ \frac{1}{\sqrt{2}}(h+iz)\end{pmatrix}$
  - Higgs self-couplings have not been measured!

$$m_h^2 = \left.\frac{d^2V}{dh^2}\right|_{h\to v} = \lambda v^2 \qquad \boxed{\lambda_{hhh}^{\rm SM} \equiv \left.\frac{d^3V}{dh^3}\right|_{h\to v} = \frac{3m_h^2}{v}}$$

  - Higgs boson couplings might be deviated from the SM.

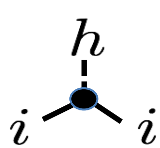

hVV, *hff*, *hhh*, …

- LHC Run-I results
  - $\boxed{\kappa_Z = 1.03^{+0.11}_{-0.11}, \kappa_W = 0.91^{+0.10}_{-0.10}}$ [ATLAS, CMS (2016)]
- Expected accuracy
  - $\Delta\kappa_V$: 2%@HL-LHC 14TeV 3ab^{-1} [ATLAS, CMS (2013)]
  - $\Delta\kappa_V$: 0.6%@ILC 250GeV 2ab^{-1}[Durieux et al. (2017)]
  - $\Delta\lambda_{hhh}$:16 (10)%@ILC 1TeV 2 (5)ab^{-1}[Fujii et al, (2015)]

Physics behind the EW symmetry breaking

- New physics is required to solve BSM phenomena

  Baryon asymmetry of the Universe, Existence of dark matter, Neutrino oscillations, Cosmic inflation,…
- BSM might be related to the extended Higgs sector

  Electroweak baryogenesis, Radiative neutrino mass models, Higgs inflation, …
- Exploring the shape of the Higgs potential is important.
  - EW phase transition at finite temperature (1st order? 2nd order ?)

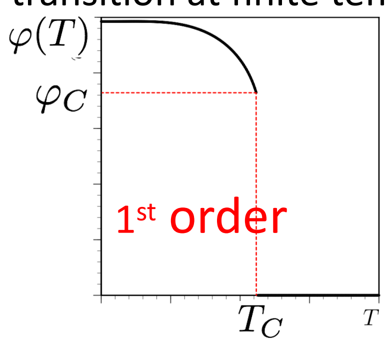

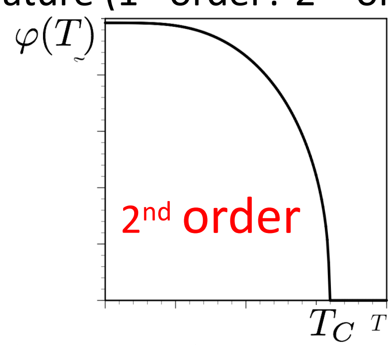

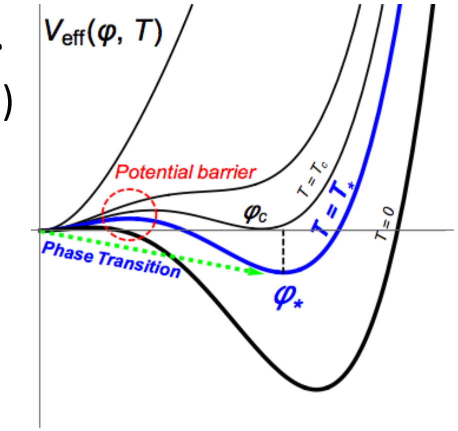

  - In order to satisfy the 3rd condition of Sakharov's conditions, strongly 1stOPT $\boxed{\varphi_*/T_* \gtrsim 1}$ (sphaleron decoupling criterion) is required in *Electroweak baryogenesis* scenario
- 1st order phase transition is not realized in the SM with m_h=125GeV.

We investigate models with extended Higgs sector.

1^{st} order phase transition

The strength of phase transition

$$V_{\rm eff} = D(T^2 - T_0^2)\varphi^2 - (\underline{ET - e})\varphi^3 + \frac{\lambda(T)}{4}\varphi^4 \quad \boxed{\frac{\varphi_c}{T_c} = \frac{2E}{\lambda}(1 - \frac{e\lambda}{ET})}$$

(Assuming one-field & high-T approx.)

1st order phase transition

See Marek Lewicki's talk

The strength of phase transition

$$V_{\rm eff} = D(T^2 - T_0^2)\varphi^2 - (ET - e)\varphi^3 + \frac{\lambda(T)}{4}\varphi^4 \qquad \boxed{\frac{\varphi_c}{T_c} = \frac{2E}{\lambda}\left(1 - \frac{e\lambda}{ET}\right)}$$

(Assuming one-field & high-T approx.)

E.g. Inert Singlet Model (a singlet scalar field with Z_2 sym.)

$$V_0 = -\mu_h^2|\Phi|^2 + \lambda_h|\Phi|^4 + \mu_S^2|S|^2 + \lambda_s|S|^4 + \lambda_{sh}|H|^2|S|^2$$

$$m_\Phi^2 \simeq \mu_S^2 + \lambda_{HS}v^2$$

$$\boxed{\frac{\Delta\lambda_{hhh}}{\lambda_{hhh}} \equiv \frac{\lambda_{hhh} - \lambda_{hhh}^{\rm SM}}{\lambda_{hhh}^{\rm SM}}}$$

$$\boxed{\lambda_{hhh} \equiv \frac{3m_h^2}{v}\left\{1 - \frac{m_t^4}{\pi^2 m_h^2 v^2} + \sum_\Phi \frac{m_\Phi^4}{12\pi^2 m_h^2 v^2}\left(1 - \frac{\mu_S^2}{m_\Phi^2}\right)\right\}}$$

Inert Singlet Model

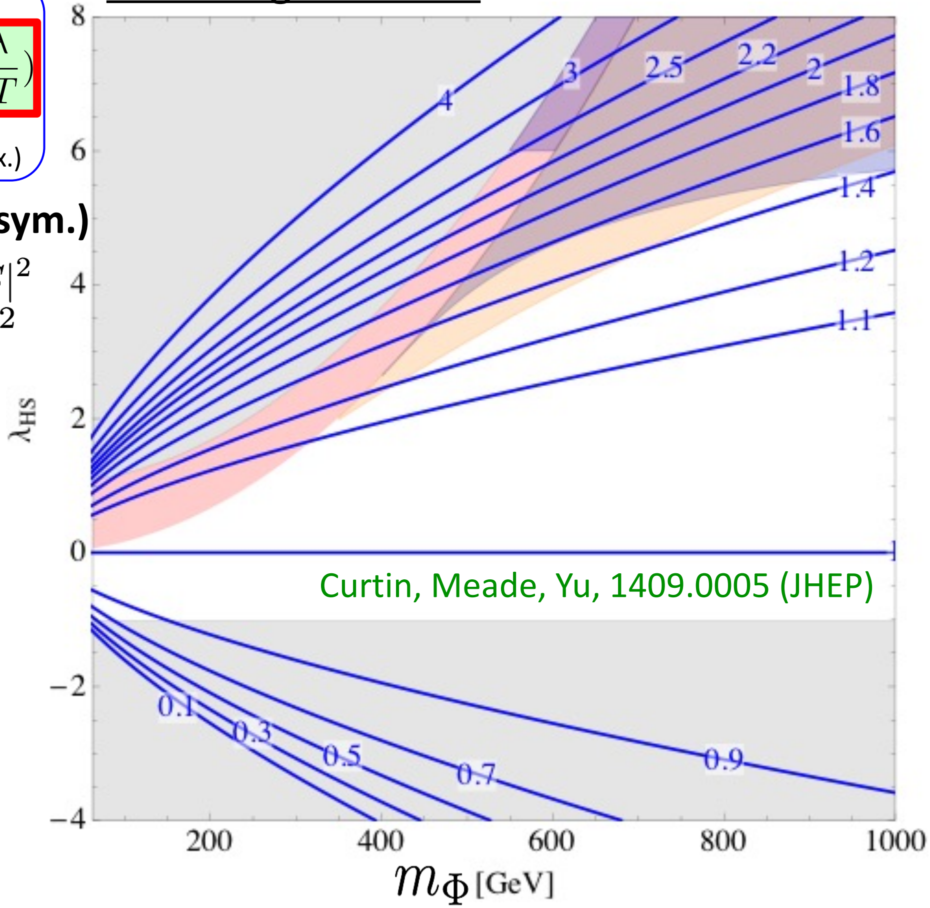

Curtin, Meade, Yu, 1409.0005 (JHEP)

1^{st} order phase transition

See Marek Lewicki's talk

The strength of phase transition

$$V_{\rm eff} = D(T^2 - T_0^2)\varphi^2 - (ET - e)\varphi^3 + \frac{\lambda(T)}{4}\varphi^4 \qquad \boxed{\frac{\varphi_c}{T_c} = \frac{2E}{\lambda}\left(1 - \frac{e\lambda}{ET}\right)}$$

(Assuming one-field & high-T approx.)

E.g. Inert Singlet Model (a singlet scalar field with Z_2 sym.)

$$V_0 = -\mu_h^2|\Phi|^2 + \lambda_h|\Phi|^4 + \mu_S^2|S|^2 + \lambda_s|S|^4 + \lambda_{sh}|H|^2|S|^2$$

$$m_\Phi^2 \simeq \mu_S^2 + \lambda_{HS}v^2$$

$$\boxed{\frac{\Delta\lambda_{hhh}}{\lambda_{hhh}} \equiv \frac{\lambda_{hhh} - \lambda_{hhh}^{\rm SM}}{\lambda_{hhh}^{\rm SM}}}$$

$$\boxed{\lambda_{hhh} \equiv \frac{3m_h^2}{v}\left\{1 - \frac{m_t^4}{\pi^2 m_h^2 v^2} + \sum_\Phi \frac{m_\Phi^4}{12\pi^2 m_h^2 v^2}\left(1 - \frac{\mu_S^2}{m_\Phi^2}\right)\right\}}$$

Inert Singlet Model

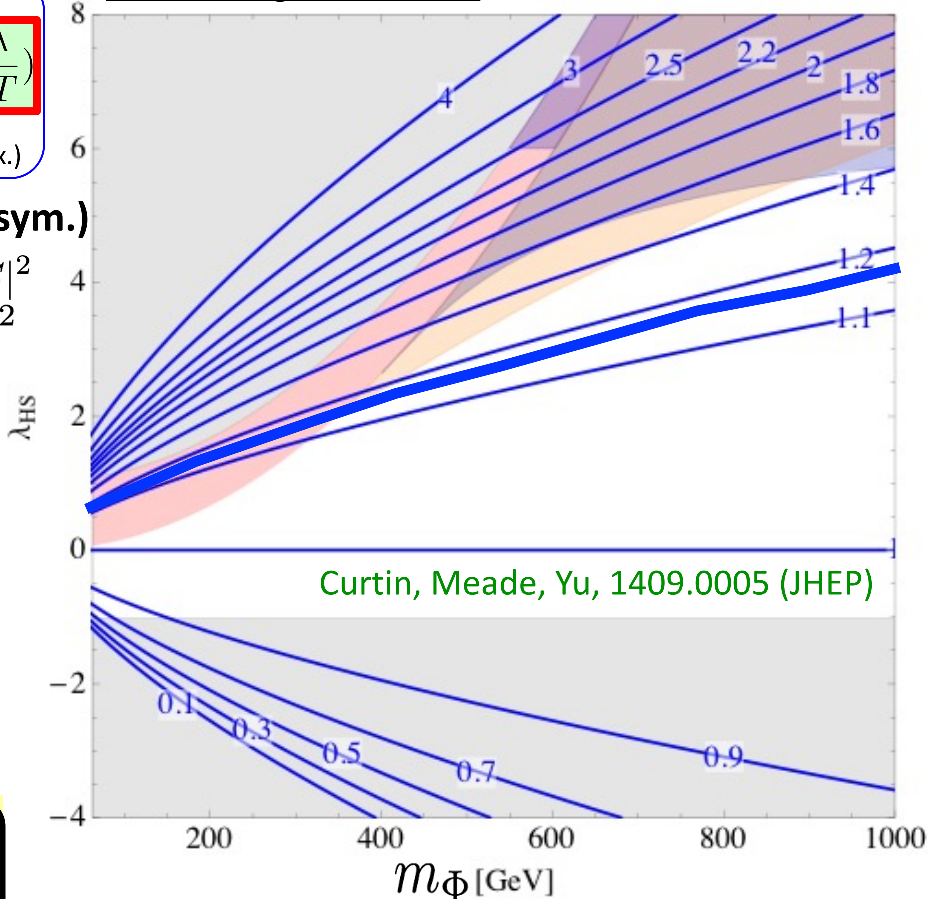

Curtin, Meade, Yu, 1409.0005 (JHEP)

Expected accuracy at collider ($\Delta\lambda_{hhh}/\lambda_{hhh}$)
- 54%@HL-LHC 14TeV 3000fb-1 [CMS-PAS-FTR-15-002],
- 27%@ILC 500GeV 4000fb-1 [Fujii et al, 1506.05992],
- 16% (10%)@ILC 1TeV 2000fb-1 (5000fb-1) [Fujii et al, 1506.05992]

1^{st} order phase transition

See Marek Lewicki's talk

The strength of phase transition

$$V_{\rm eff} = D(T^2 - T_0^2)\varphi^2 - (ET - e)\varphi^3 + \frac{\lambda(T)}{4}\varphi^4 \qquad \boxed{\frac{\varphi_c}{T_c} = \frac{2E}{\lambda}\left(1 - \frac{e\lambda}{ET}\right)}$$

(Assuming one-field & high-T approx.)

E.g. Inert Singlet Model (a singlet scalar field with Z_2 sym.)

$$V_0 = -\mu_h^2|\Phi|^2 + \lambda_h|\Phi|^4 + \mu_S^2|S|^2 + \lambda_s|S|^4 + \lambda_{sh}|H|^2|S|^2$$

$$m_\Phi^2 \simeq \mu_S^2 + \lambda_{HS} v^2$$

$$\frac{\Delta\lambda_{hhh}}{\lambda_{hhh}} \equiv \frac{\lambda_{hhh} - \lambda_{hhh}^{\rm SM}}{\lambda_{hhh}^{\rm SM}}$$

$$\lambda_{hhh} \equiv \frac{3m_h^2}{v}\left\{1 - \frac{m_t^4}{\pi^2 m_h^2 v^2} + \sum_\Phi \frac{m_\Phi^4}{12\pi^2 m_h^2 v^2}\left(1 - \frac{\mu_S^2}{m_\Phi^2}\right)^3\right\}$$

Inert Singlet Model

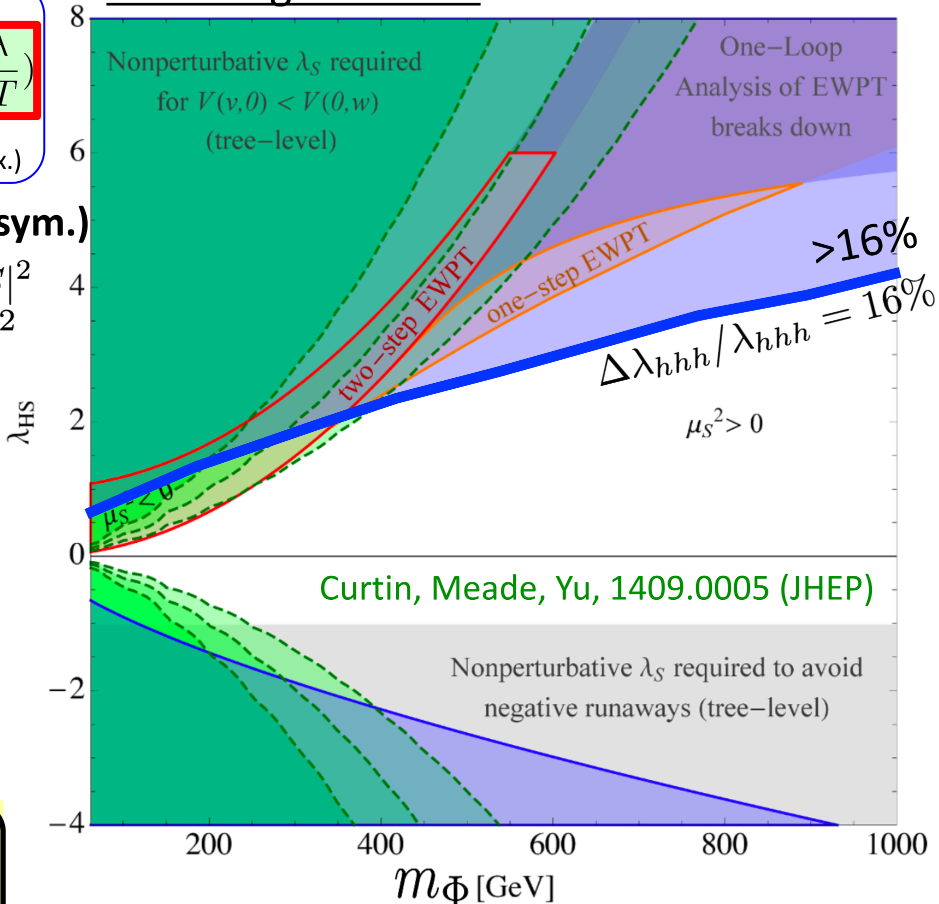

Expected accuracy at collider ($\Delta\lambda_{hhh}/\lambda_{hhh}$)
- 54%@HL-LHC 14TeV 3000fb-1 [CMS-PAS-FTR-15-002],
- 27%@ILC 500GeV 4000fb-1 [Fujii et al, 1506.05992],
- 16% (10%)@ILC 1TeV 2000fb-1 (5000fb-1) [Fujii et al, 1506.05992]

1^{st} order phase transition

See Marek Lewicki's talk

The strength of phase transition

$$V_{\rm eff} = D(T^2 - T_0^2)\varphi^2 - \underline{(ET - e)}\varphi^3 + \frac{\lambda(T)}{4}\varphi^4 \qquad \boxed{\frac{\varphi_c}{T_c} = \frac{2E}{\lambda}\left(1 - \frac{e\lambda}{ET}\right)}$$

(Assuming one-field & high-T approx.)

E.g. Inert Singlet Model (a singlet scalar field with Z_2 sym.)

$$V_0 = -\mu_h^2|\Phi|^2 + \lambda_h|\Phi|^4 + \mu_S^2|S|^2 + \lambda_s|S|^4 + \lambda_{sh}|H|^2|S|^2$$

$$m_\Phi^2 \simeq \mu_S^2 + \lambda_{HS}v^2$$

$$\frac{\Delta\lambda_{hhh}}{\lambda_{hhh}} \equiv \frac{\lambda_{hhh} - \lambda_{hhh}^{\rm SM}}{\lambda_{hhh}^{\rm SM}}$$

$$\lambda_{hhh} \equiv \frac{3m_h^2}{v}\left\{1 - \frac{m_t^4}{\pi^2 m_h^2 v^2} + \sum_\Phi \frac{m_\Phi^4}{12\pi^2 m_h^2 v^2}\left(1 - \frac{\mu_S^2}{m_\Phi^2}\right)^3\right\}$$

Correlation!!

Enhanced by $M \to 0$ (large λ_{HS}) limit

One-step EWPT

$$E = \frac{1}{12\pi v^3}\left\{6m_{W^\pm}^3 + 3m_Z^3 + \sum_\Phi m_\Phi^3\left(1 - \frac{\mu_S^2}{m_\Phi^2}\right)^3\left(1 + \frac{3}{2}\frac{\mu_S^2}{m_\Phi^2}\right)\right\}$$

Expected accuracy at collider ($\Delta\lambda_{hhh}/\lambda_{hhh}$)
- 54%@HL-LHC 14TeV 3000fb-1 [CMS-PAS-FTR-15-002],
- 27%@ILC 500GeV 4000fb-1 [Fujii et al, 1506.05992],
- 16% (10%)@ILC 1TeV 2000fb-1 (5000fb-1) [Fujii et al, 1506.05992]

Inert Singlet Model

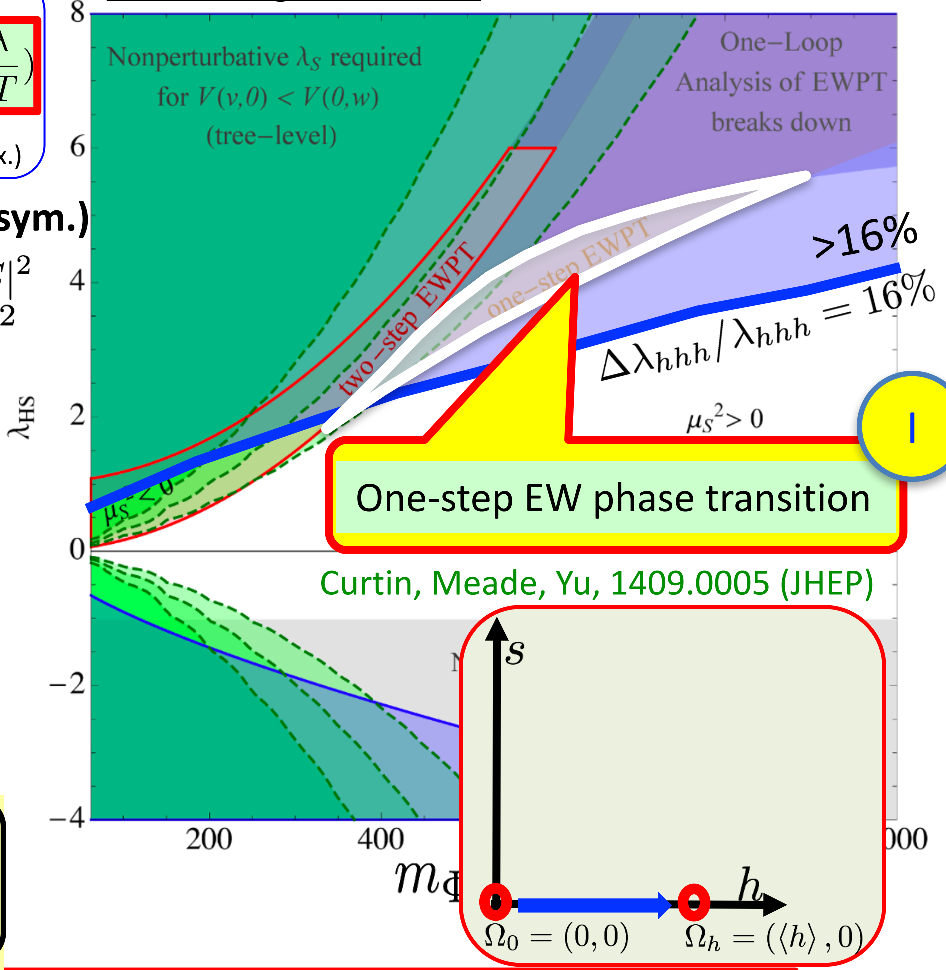

Curtin, Meade, Yu, 1409.0005 (JHEP)

Large deviation in the *hhh* coupling is required! → EWPT can be tested at future colliders!

1st order phase transition

See Marek Lewicki's talk

The strength of phase transition

$$V_{\rm eff} = D(T^2 - T_0^2)\varphi^2 - \underline{(ET - e)}\varphi^3 + \frac{\lambda(T)}{4}\varphi^4 \qquad \boxed{\frac{\varphi_c}{T_c} = \frac{2E}{\lambda}\left(1 - \frac{e\lambda}{ET}\right)}$$

(Assuming one-field & high-T approx.)

E.g. Inert Singlet Model (a singlet scalar field with Z_2 sym.)

$$V_0 = -\mu_h^2|\Phi|^2 + \lambda_h|\Phi|^4 + \mu_S^2|S|^2 + \lambda_s|S|^4 + \lambda_{sh}|H|^2|S|^2$$

$$\frac{\Delta\lambda_{hhh}}{\lambda_{hhh}} \equiv \frac{\lambda_{hhh} - \lambda_{hhh}^{\rm SM}}{\lambda_{hhh}^{\rm SM}}$$

$$\lambda_{hhh} \equiv \frac{3m_h^2}{v}\left\{1 - \frac{m_t^4}{\pi^2 m_h^2 v^2} + \sum_\Phi \frac{m_\Phi^4}{12\pi^2 m_h^2 v^2}\left(1 - \frac{\mu_S^2}{m_\Phi^2}\right)\right\}$$

II

Two-step EW phase transition

Correlation!!

Enhanced by $M \to 0$ (large λ_{HS}) limit

One-step EWPT

$$E = \frac{1}{12\pi v^3}\left\{6m_{W^\pm}^3 + 3m_Z^3 + \sum_\Phi m_\Phi^3\left(1 - \frac{\mu_S^2}{m_\Phi^2}\right)^3\left(1 + \frac{3}{2}\frac{\mu_S^2}{m_\Phi^2}\right)\right\}$$

Expected accuracy at collider ($\Delta\lambda_{hhh}/\lambda_{hhh}$)

- 54%@HL-LHC 14TeV 3000fb-1 [CMS-PAS-FTR-15-002],
- 27%@ILC 500GeV 4000fb-1 [Fujii et al, 1506.05992],
- 16% (10%)@ILC 1TeV 2000fb-1 (5000fb-1) [Fujii et al, 1506.05992]

Inert Singlet Model

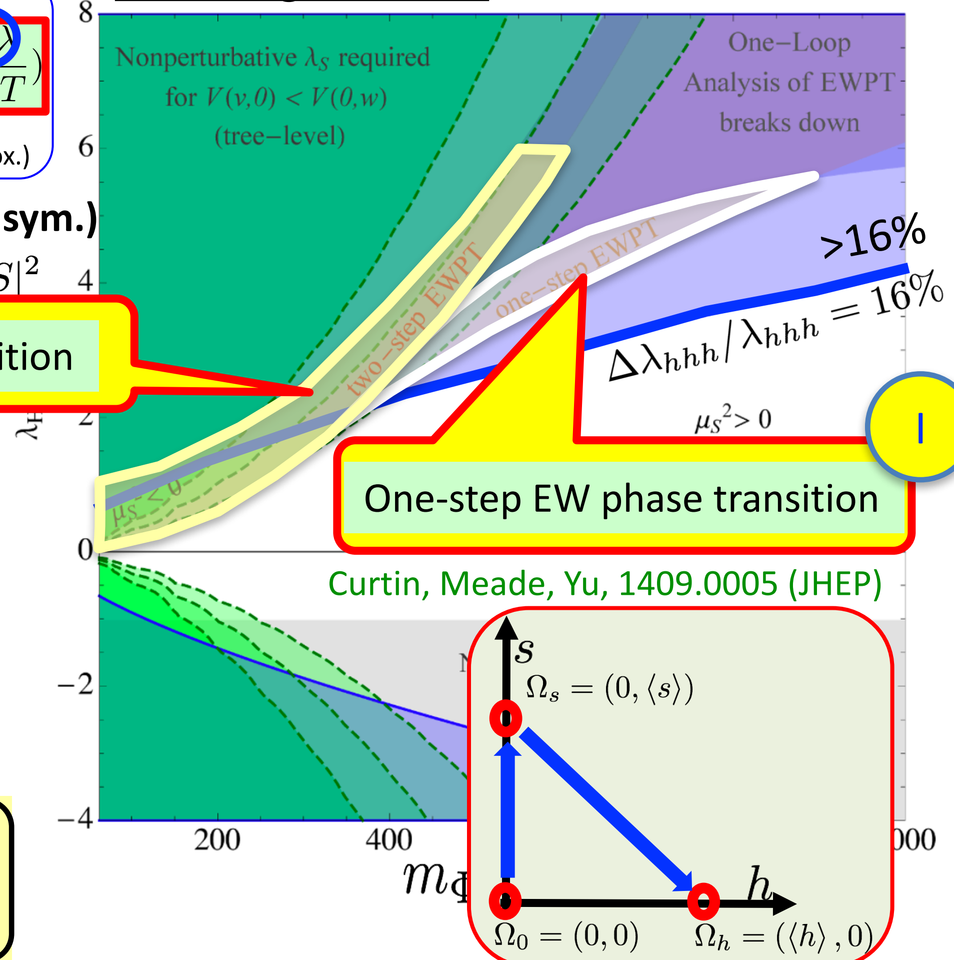

Curtin, Meade, Yu, 1409.0005 (JHEP)

Large deviation in the *hhh* coupling is required! → EWPT can be tested at future colliders!

I

(N, m_s) may be determined from GWs

O(N) singlet model with the mass m_s

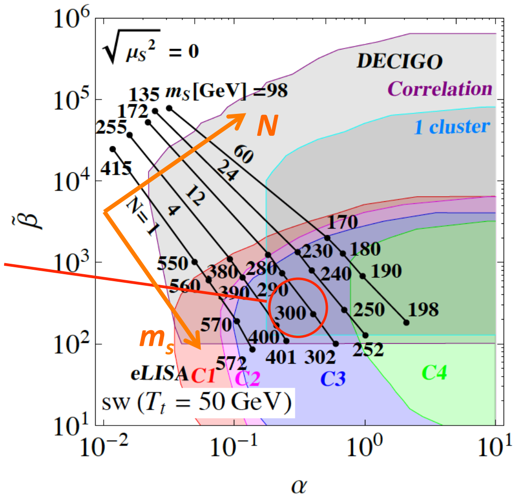

Sensitivities

eLISA arXiv:1512.06239

DECIGO, Class. Quant. Grav. 28, 094011 (2011)

If α and β are determined with a resolution, We may be able to fingerprint the model with (N, m_S)

M. Kakizaki, SK, T. Matsui, Phys. Rev. D92 (2015) no.11,115007

See Shinya Kanemura's talk

Synergy of various measurements

hVV/hff ← HL-LHC
hhh ← ILC
GWs ← LISA

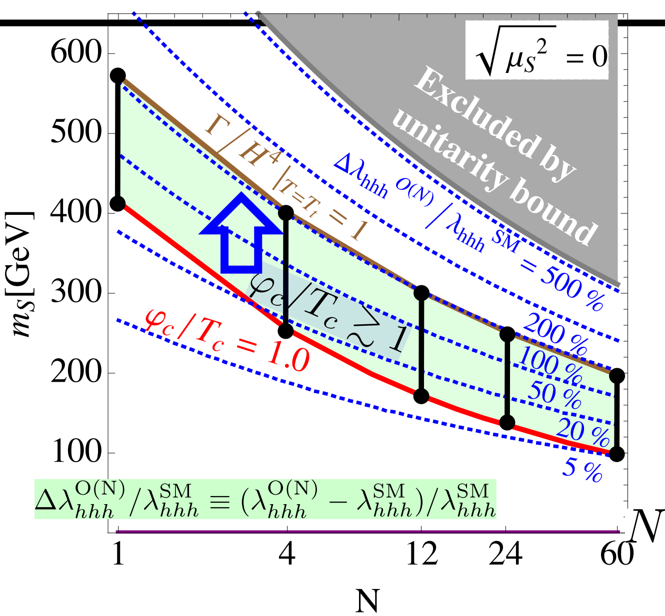

II

$\kappa = \kappa_V = \kappa_f$

$= \cos\theta$

Precision measurement at ILC, FCCee

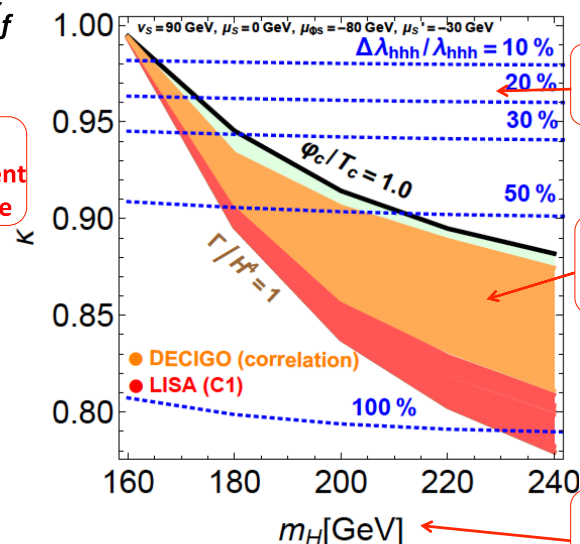

Self-coupling *hhh* measurement at ILC

Measurement of Gravitational Waves at LISA/DECIGO

Direct searches of the second Higgs at LHC

K. Hashino, M. Kakizaki, S.K., T. Matsui, P. Ko, Phys. Lett. B 766, 49 (2017)

1^{st} order phase transition

The strength of phase transition $\frac{\varphi_c}{T_c} = \frac{2E}{\lambda}\left(1 - \frac{e\lambda}{ET}\right)$

$$V_{\rm eff} = D(T^2 - T_0^2)\varphi^2 - (ET - e)\varphi^3 + \frac{\lambda(T)}{4}\varphi^4$$

(Assuming one-field & high-T approx.)

E.g. Inert Singlet Model (a singlet scalar field with Z_2 sym.)

$$V_0 = -\mu_h^2|\Phi|^2 + \lambda_h|\Phi|^4 + \mu_S^2|S|^2 + \lambda_s|S|^4 + \lambda_{sh}|H|^2|S|^2$$

$$\frac{\Delta\lambda_{hhh}}{\lambda_{hhh}} \equiv \frac{\lambda_{hhh} - \lambda_{hhh}^{\rm SM}}{\lambda_{hhh}^{\rm SM}}$$

$$\lambda_{hhh} \equiv \frac{3m_h^2}{v}\left\{1 - \frac{m_t^4}{\pi^2 m_h^2 v^2} + \sum_\Phi \frac{m_\Phi^4}{12\pi^2 m_h^2 v^2}\left(1 - \frac{\mu_S^2}{m_\Phi^2}\right)\right\}$$

Correlation!!

Enhanced by $M \to 0$ (large λ_{HS}) limit

One-step EWPT

$$E = \frac{1}{12\pi v^3}\left\{6m_{W^\pm}^3 + 3m_Z^3 + \sum_\Phi m_\Phi^3\left(1 - \frac{\mu_S^2}{m_\Phi^2}\right)^3\left(1 + \frac{3}{2}\frac{\mu_S^2}{m_\Phi^2}\right)\right\}$$

II Two-step EW phase transition

Expected accuracy at collider ($\Delta\lambda_{hhh}/\lambda_{hhh}$)
- 54%@HL-LHC 14TeV 3000fb-1 [CMS-PAS-FTR-15-002],
- 27%@ILC 500GeV 4000fb-1 [Fujii et al, 1506.05992],
- 16% (10%)@ILC 1TeV 2000fb-1 (5000fb-1) [Fujii et al, 1506.05992]

Inert Singlet Model

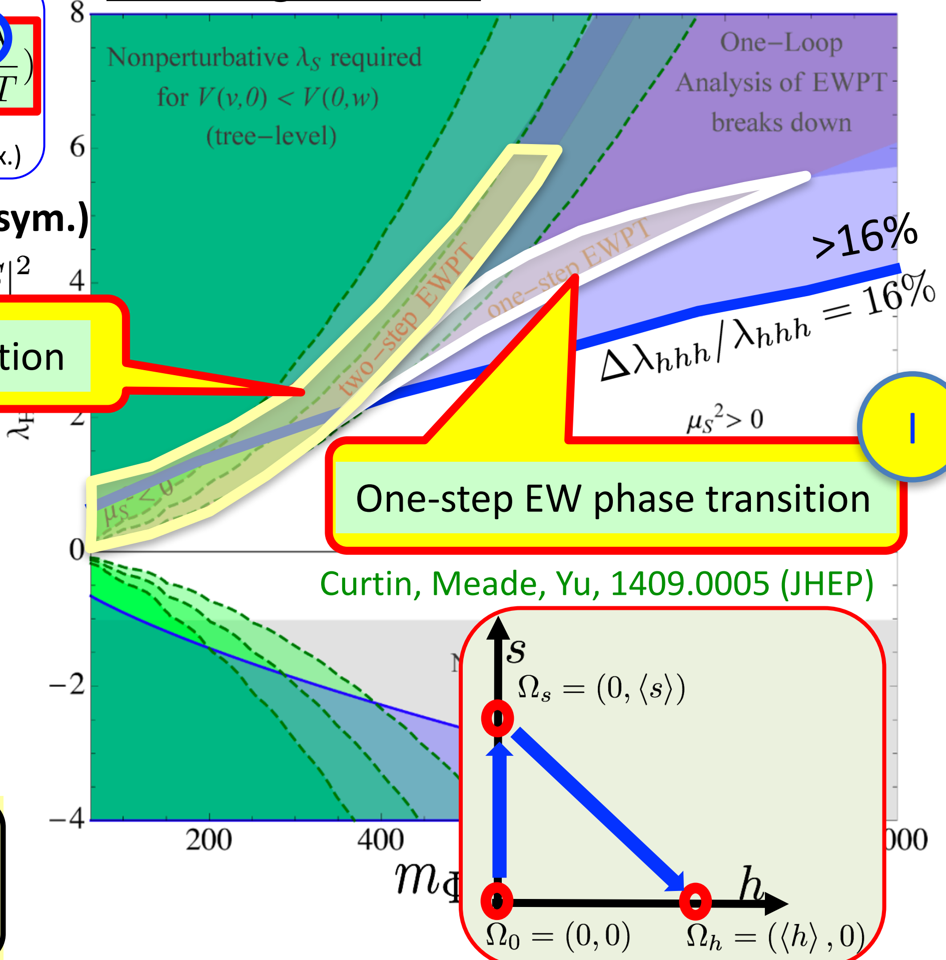

Curtin, Meade, Yu, 1409.0005 (JHEP)

Large deviation in the *hhh* coupling is required! → EWPT can be tested at future colliders!

1^{st} order phase transition

The strength of phase transition

$$\frac{\varphi_c}{T_c} = \frac{2E}{\lambda}\left(1 - \frac{e\lambda}{ET}\right)$$

$$V_{\rm eff} = D(T^2 - T_0^2)\varphi^2 - (ET - e)\varphi^3 + \frac{\lambda(T)}{4}\varphi^4$$

(Assuming one-field & high-T approx.)

E.g. Inert Singlet Model (a singlet scalar field with Z_2 sym.)

$$V_0 = -\mu_h^2|\Phi|^2 + \lambda_h|\Phi|^4 \ldots |S|^2 + \lambda_s|S|^4 + \lambda_{sh}|H|^2|S|^2$$

$$\frac{\Delta\lambda_{hhh}}{\lambda_{hhh}} \equiv \frac{\lambda_{hhh} - \lambda_{hhh}^{\rm SM}}{\lambda_{hhh}^{\rm SM}}$$

$$\lambda_{hhh} \equiv \frac{3m_h^2}{v}\left\{1 - \frac{m_t^4}{\pi^2 m_h^2 v^2} + \sum_\Phi \frac{m_\Phi^4}{12\pi^2 m_h^2 v^2}\left(1 - \frac{\mu_S^2}{m_\Phi^2}\right)^3\right\}$$

Correlation!!

...) limit

II

Two-step EW phase transition

III

Two-step EW phase transition

※ In this region, Higgs couplings does not deviate from the SM (nightmare scenario)

- 27%@ILC 500GeV 4000fb-1 [Fujii et al, 1506.05992],
- 16% (10%)@ILC 1TeV 2000fb-1 (5000fb-1) [Fujii et al, 1506.05992]

Inert Singlet Model

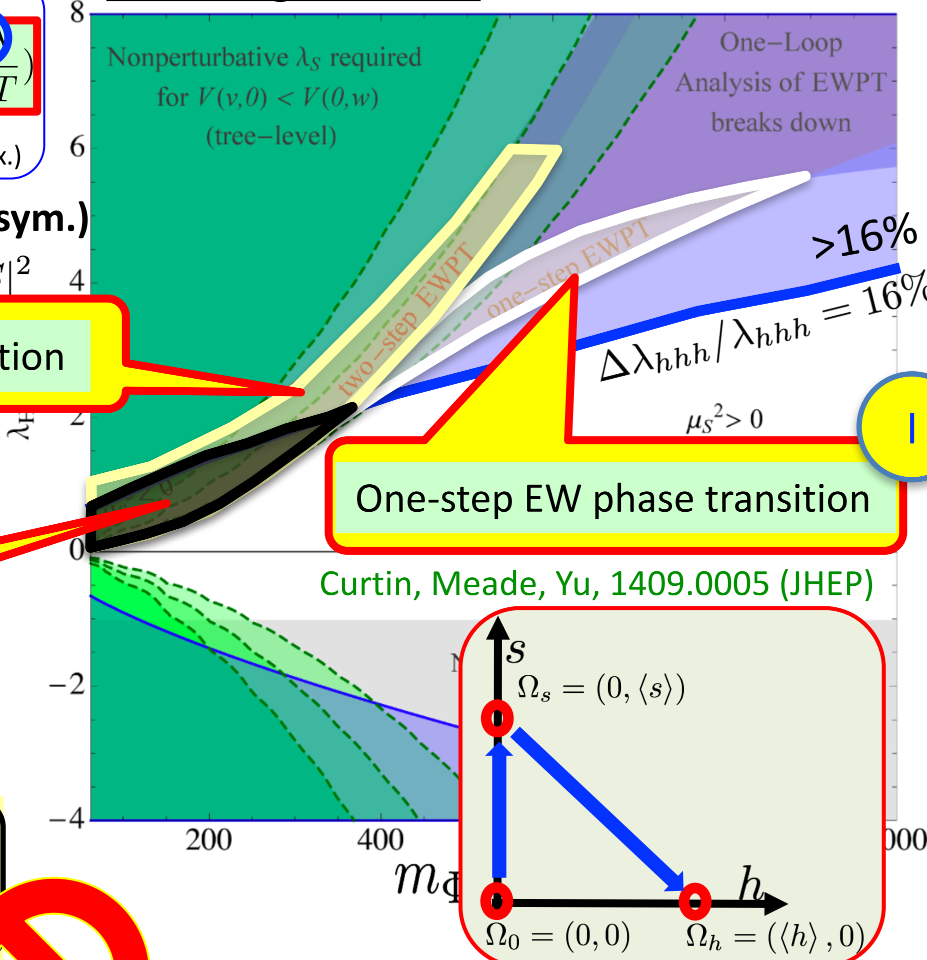

I

One-step EW phase transition

Curtin, Meade, Yu, 1409.0005 (JHEP)

Large deviation in the *hhh* coupling is requir... EWPT can be tested at future colliders!

III

Nightmare scenario

- Potential barrier with 1stOPT can be realized by multi-step PT even if the Higgs couplings do not deviate from SM.

- In the models with the unbroken discrete symmetry (such as Z_2, Z_3, …) or mixing angle=0, it is difficult to test at colliders.

- We expect the observations of the gravitational waves as a new technique to detect the signal of the 1stOPT.

Gravitational waves

～ Probing the Higgs potential by GW observations ～

Sensitivity of GW detectors

http://rhcole.com/apps/GWplotter/

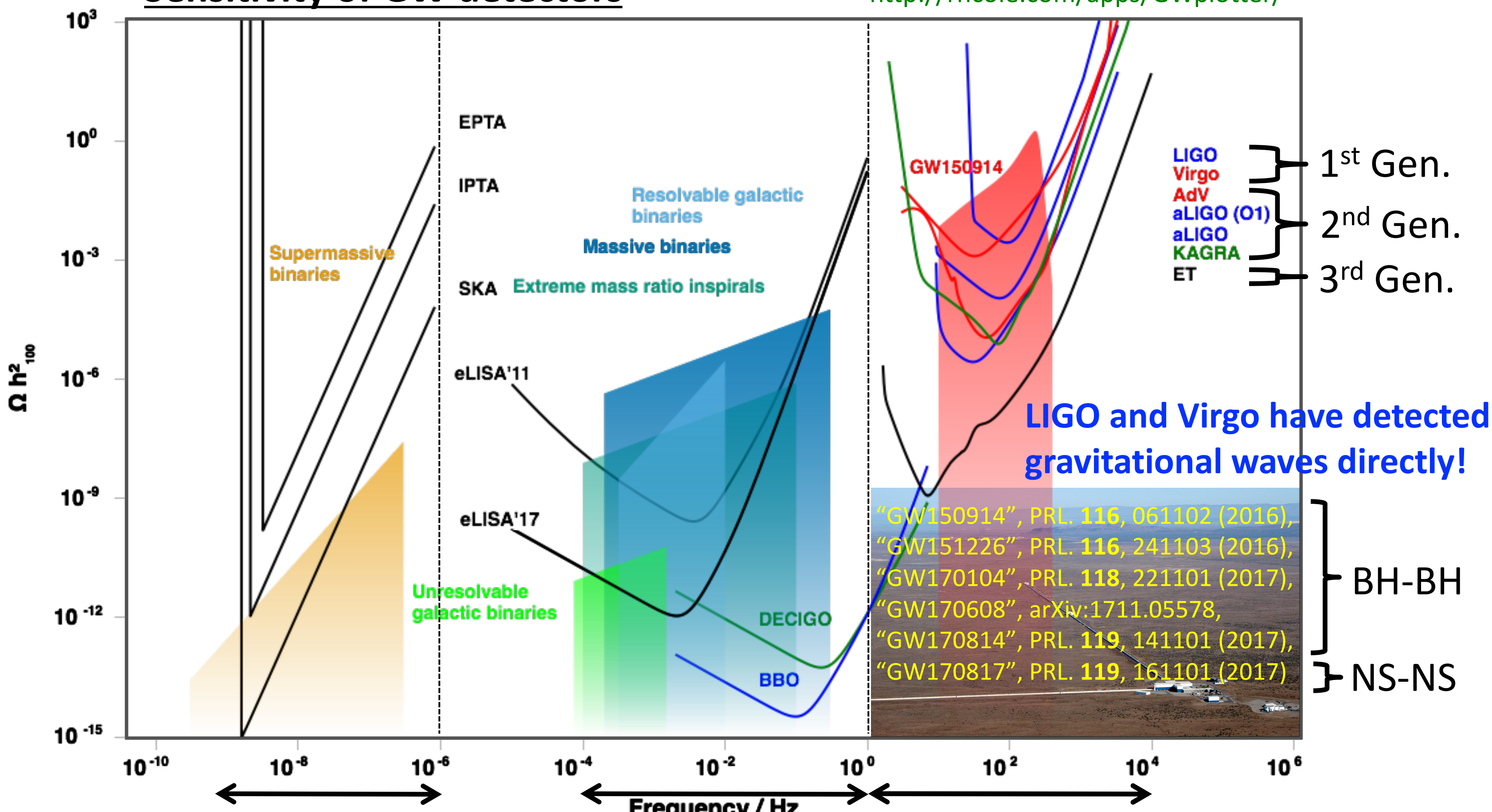

Pulsar Timing Array (PTA)

Space-based interferometers

Ground-based interferometers

Gravitational waves

～ Probing the Higgs potential by GW observations ～

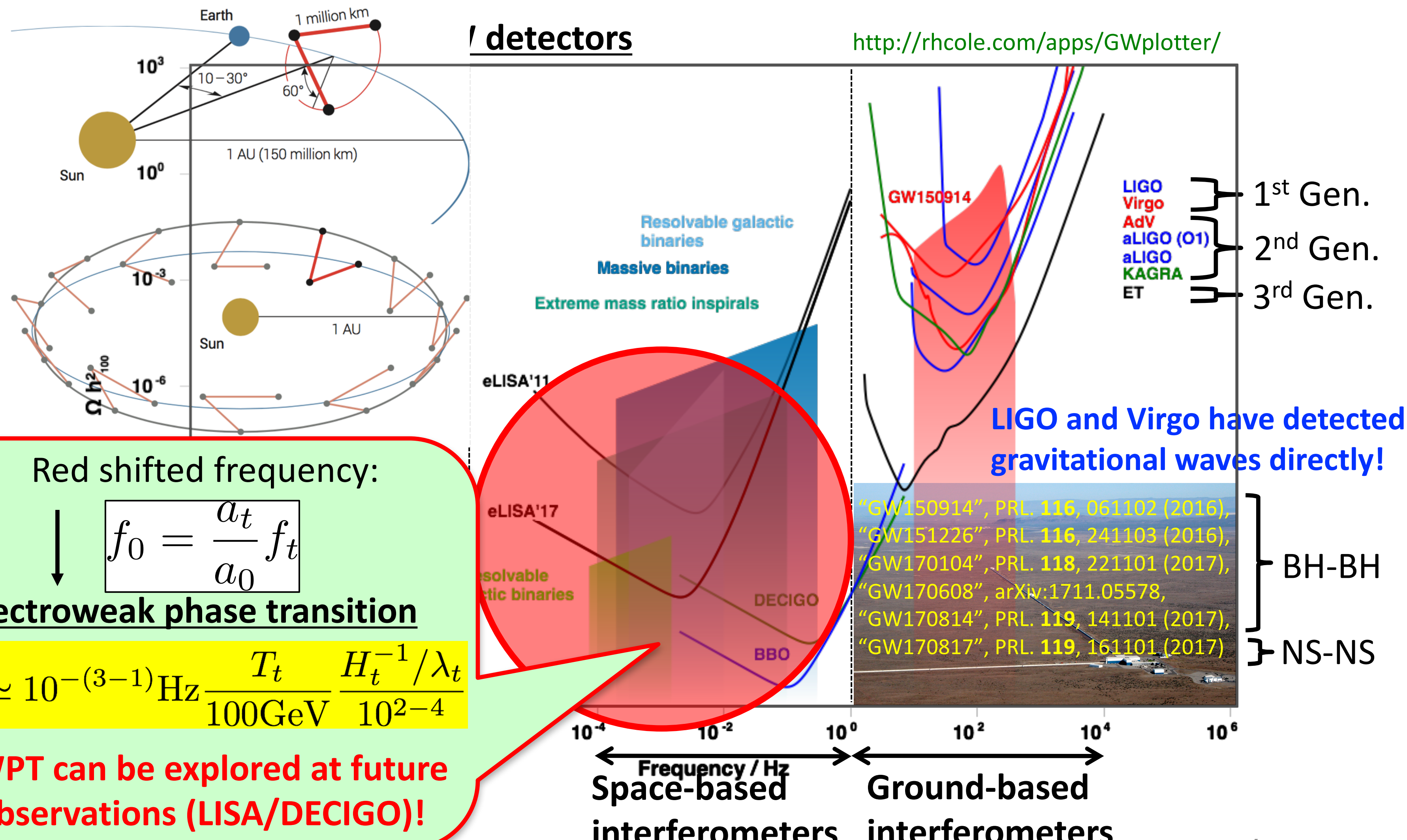

Red shifted frequency:

$$\boxed{f_0 = \frac{a_t}{a_0} f_t}$$

Electroweak phase transition

$$f_0 \simeq 10^{-(3-1)}\mathrm{Hz}\frac{T_t}{100\mathrm{GeV}}\frac{H_t^{-1}/\lambda_t}{10^{2-4}}$$

EWPT can be explored at future observations (LISA/DECIGO)!

GWs from 1stOPT

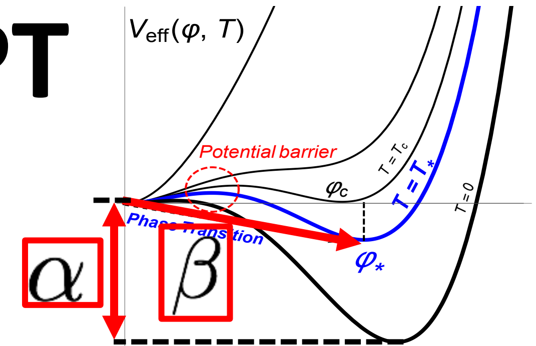

Characteristic parameters of 1stOPT

- α is defined as $\alpha \equiv \left.\dfrac{\epsilon}{\rho_{\rm rad}}\right|_{T=T_t}$. ($\rho_{\rm rad}$ is energy density of rad.)
  - Latent heat: $\epsilon(T) \equiv -\Delta V_{\rm eff}(\varphi_B(T), T) + T\dfrac{\partial \Delta V_{\rm eff}(\varphi_B(T))}{\partial T}$

  α ~ "Normalized difference of the potential minima"

- β is defined as $\beta \equiv \left.\dfrac{1}{\Gamma}\dfrac{d\Gamma}{dt}\right|_{t=t_t}$. → $\tilde{\beta}\left(\equiv \dfrac{\beta}{H_t}\right) = T_t \left.\dfrac{d(S_3(T)/T)}{dT}\right|_{T=T_t}$
  - Bubble nucleation rate : $\Gamma(T) \simeq T^4 e^{-\frac{S_3(T)}{T}}$
  - 3-dim. Euclidean action: $S_3(T) = \int dr^3 \left\{\frac{1}{2}\left(\vec{\nabla}\varphi\right)^2 + V_{\rm eff}(\varphi, T)\right\}$

  β^{-1} ~ "Transition time"

$V_{\rm eff}(\varphi, T)$ (Model)

↓

$\alpha,\ \tilde{\beta}$ @T=T_t

↓ Prediction*

$\Omega_{\rm GW}(f)h^2$ (Observable)

Relic abundance of GWs

$$\boxed{\Omega_{\rm GW} \propto \left(\frac{H}{\beta}\right)^n \left(\frac{\kappa\alpha}{1+\alpha}\right)^m}$$

- **"Sound waves" (Compressional plasma)** [n=1, m=2]
- **"Bubble collision" (Envelope approximation)** [n=2, m=2]
- **"Magnetohydrodynamic turbulence in the plasma"** [n=2, m=3/2]

→Exact formulae based on the numerical simulation are shown in C. Caprini *et al.*, JCAP**1604**, 001 (2016)

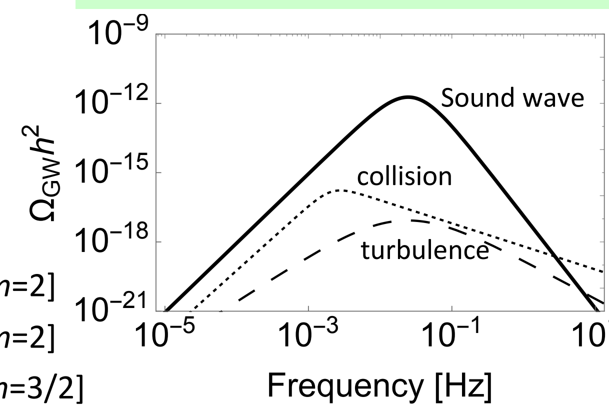

GWs from 1stOPT

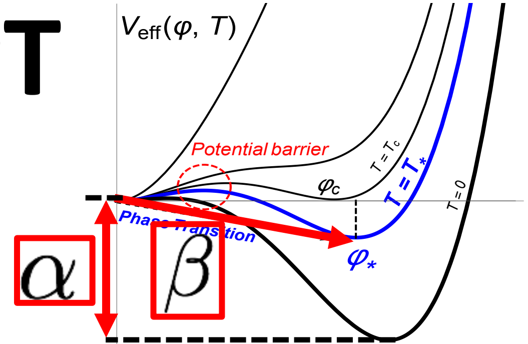

$V_{\rm eff}(\varphi, T)$ (Model)

↓

$\alpha,\ \tilde{\beta}$ @T=T$_t$

↓ Prediction*

$\Omega_{\rm GW}(f)h^2$ (Observable)

Characteristic parameters of 1stOPT

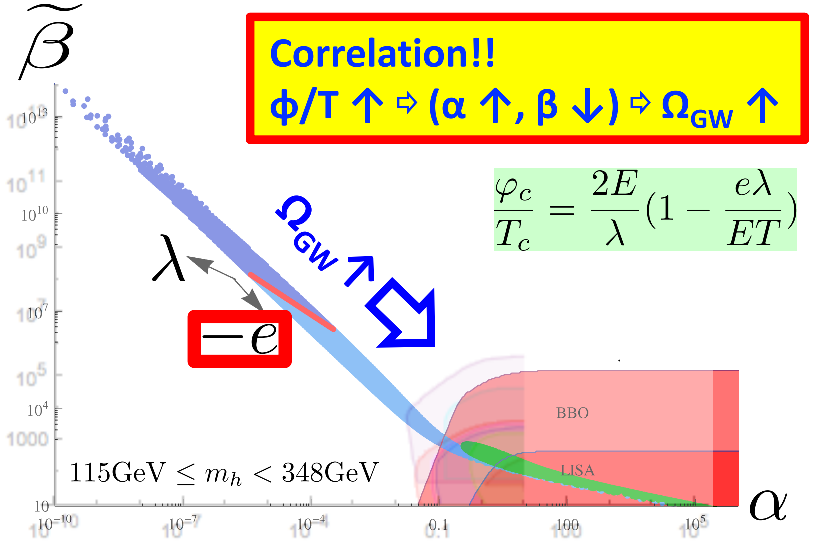

J. Kehayias and S. Profumo, JCAP**1003**, 003 (2010)

Relic abundance of GWs

$$\Omega_{\rm GW} \propto \left(\frac{H}{\beta}\right)^n \left(\frac{\kappa\alpha}{1+\alpha}\right)^m$$

- **"Sound waves" (Compressional plasma)** [*n*=1, *m*=2]
- **"Bubble collision" (Envelope approximation)** [*n*=2, *m*=2]
- **"Magnetohydrodynamic turbulence in the plasma"** [*n*=2, *m*=3/2]

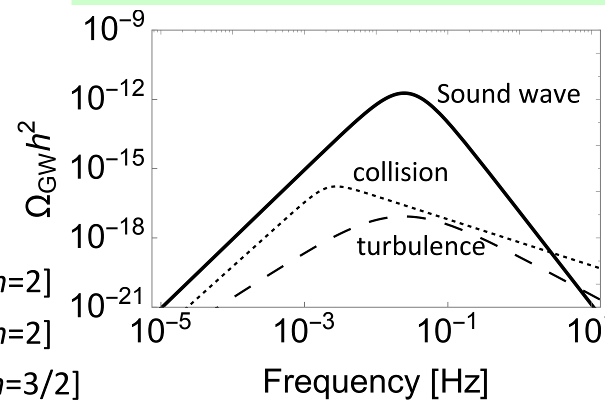

→Exact formulae based on the numerical simulation are shown in C. Caprini *et al.*, JCAP**1604**, 001 (2016)

Z_3-symmetric model

- Higgs sector [$A_s \to 0$: Z_2 model limit]

$$V_0 = -\mu_h^2|\Phi|^2 + \lambda_h|\Phi|^4 - \mu_s^2|S|^2 + \lambda_s|S|^4 + \lambda_{sh}|H|^2|S|^2 + \sqrt{2}\left(\frac{A_s}{3}S^3 + \text{h.c.}\right)$$

  - complex singlet scalar: $S \to e^{i2w}S$ with $w = \pi/3$

- Phase transition patterns
  - One-step ($\mu_s^2 > 0$, largeλ_{sh})
    $\Omega_0 \to \Omega_h$
  - Two-step ($\mu_s^2 < 0$)
    $\Omega_0 \to \Omega_s \to \Omega_h$
  - Three-step
    $\Omega_0 \to \Omega_s \to \Omega_{sh} \to \Omega_h$

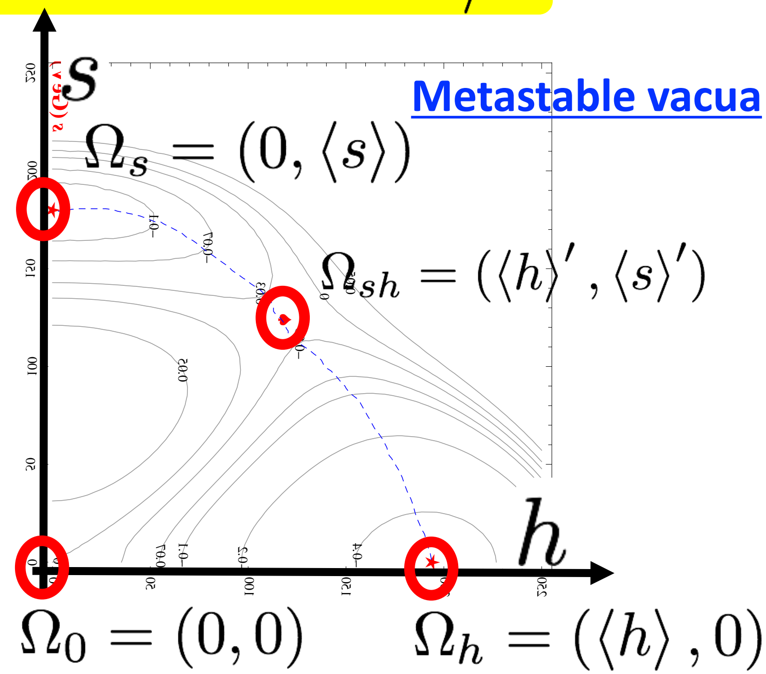

Z_3-symmetric model

- Higgs sector [$A_s \to 0$: Z_2 model limit]

$$V_0 = -\mu_h^2|\Phi|^2 + \lambda_h|\Phi|^4 - \mu_s^2|S|^2 + \lambda_s|S|^4 + \lambda_{sh}|H|^2|S|^2 + \sqrt{2}\left(\frac{A_s}{3}S^3 + \text{h.c.}\right)$$

  – complex singlet scalar: $S \to e^{i2w}S$ with $w = \pi/3$

- Phase transition patterns
  – One-step ($\mu_s^2 > 0$, largeλ_{sh})
  $\Omega_0 \to \Omega_h$

Metastable vacua

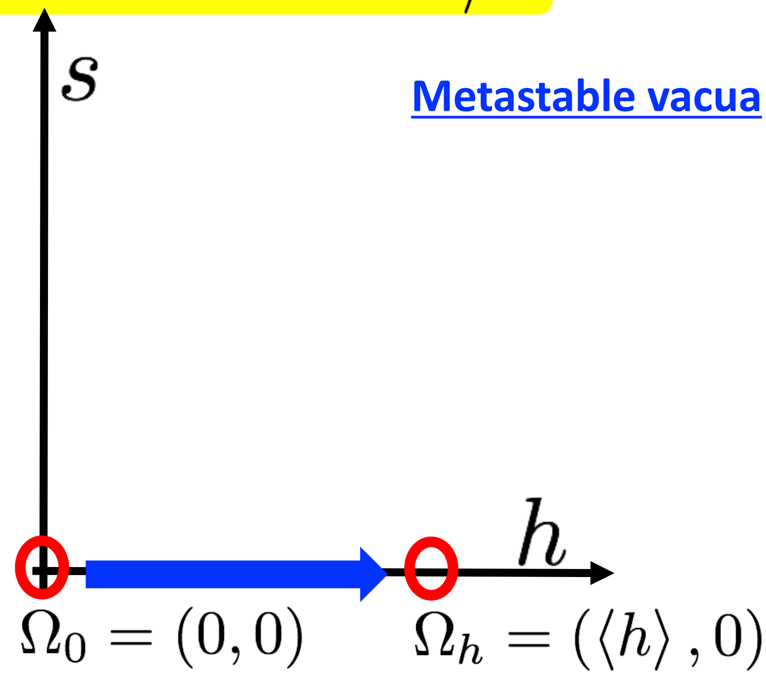

Z_3-symmetric model

- Higgs sector [$A_s \to 0$: Z_2 model limit]

$$V_0 = -\mu_h^2|\Phi|^2 + \lambda_h|\Phi|^4 - \mu_s^2|S|^2 + \lambda_s|S|^4 + \lambda_{sh}|H|^2|S|^2 + \sqrt{2}\left(\frac{A_s}{3}S^3 + \text{h.c.}\right)$$

  – complex singlet scalar: $S \to e^{i2w}S$ with $w = \pi/3$

- Phase transition patterns

  – Two-step $(\mu_s^2 < 0)$
  $\Omega_0 \to \Omega_s \to \Omega_h$

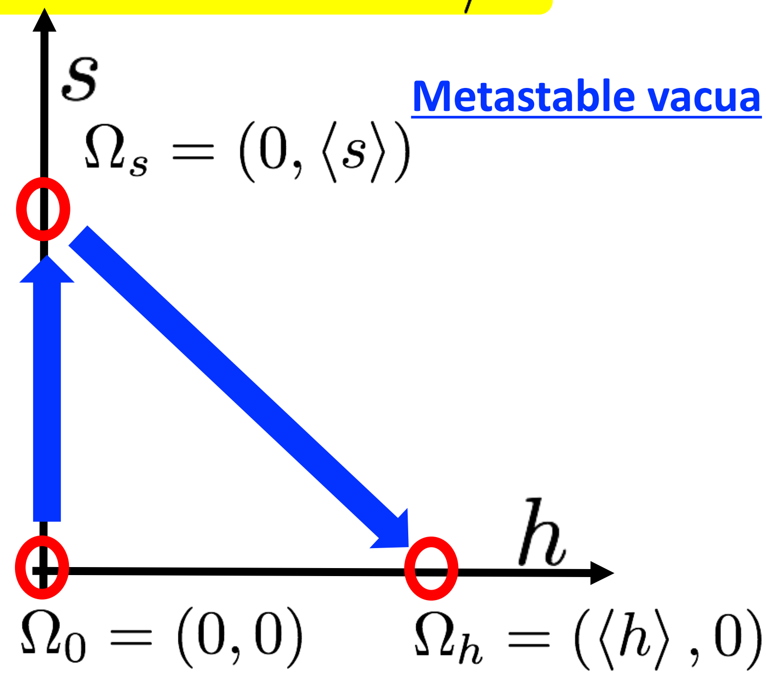

Z_3-symmetric model

- Higgs sector [$A_s \to 0$: Z_2 model limit]

$$V_0 = -\mu_h^2|\Phi|^2 + \lambda_h|\Phi|^4 - \mu_s^2|S|^2 + \lambda_s|S|^4 + \lambda_{sh}|H|^2|S|^2 + \sqrt{2}\left(\frac{A_s}{3}S^3 + \text{h.c.}\right)$$

  - complex singlet scalar: $S \to e^{i2w}S$ with $w = \pi/3$

- Phase transition patterns

  - Three-step

$$\Omega_0 \to \Omega_s \to \Omega_{sh} \to \Omega_h$$

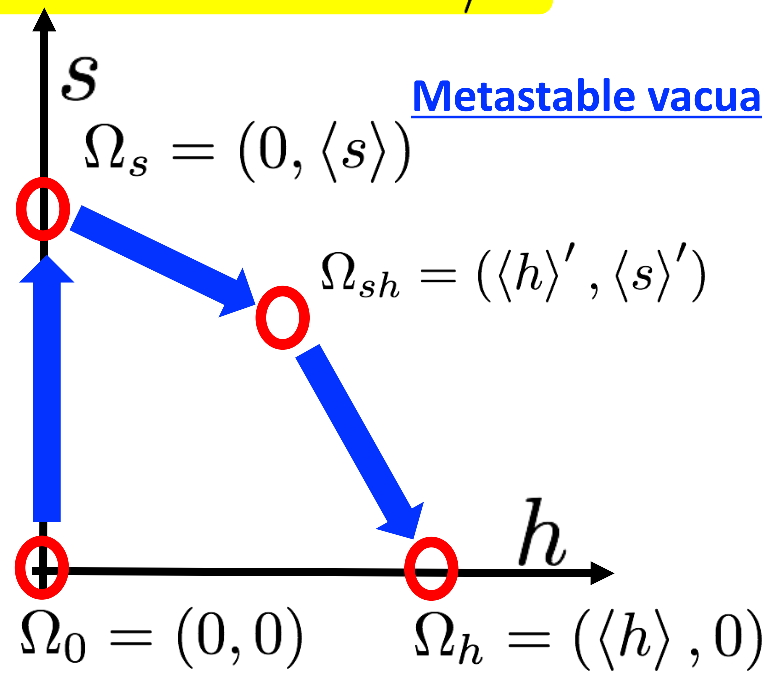

Z_3-symmetric model

- Higgs sector [$A_s \to 0$: Z_2 model limit]

$$V_0 = -\mu_h^2|\Phi|^2 + \lambda_h|\Phi|^4 - \mu_s^2|S|^2 + \lambda_s|S|^4 + \lambda_{sh}|H|^2|S|^2 + \sqrt{2}\left(\frac{A_s}{3}S^3 + \text{h.c.}\right)$$

  – complex singlet scalar: $S \to e^{i2w}S$ with $w = \pi/3$

- Phase transition patterns
  – One-step ($\mu_s^2 > 0$, largeλ_{sh})
  $$\Omega_0 \to \Omega_h$$
  – Two-step ($\mu_s^2 < 0$)
  $$\Omega_0 \to \Omega_s \to \Omega_h$$
  – Three-step
  $$\Omega_0 \to \Omega_s \to \Omega_{sh} \to \Omega_h$$

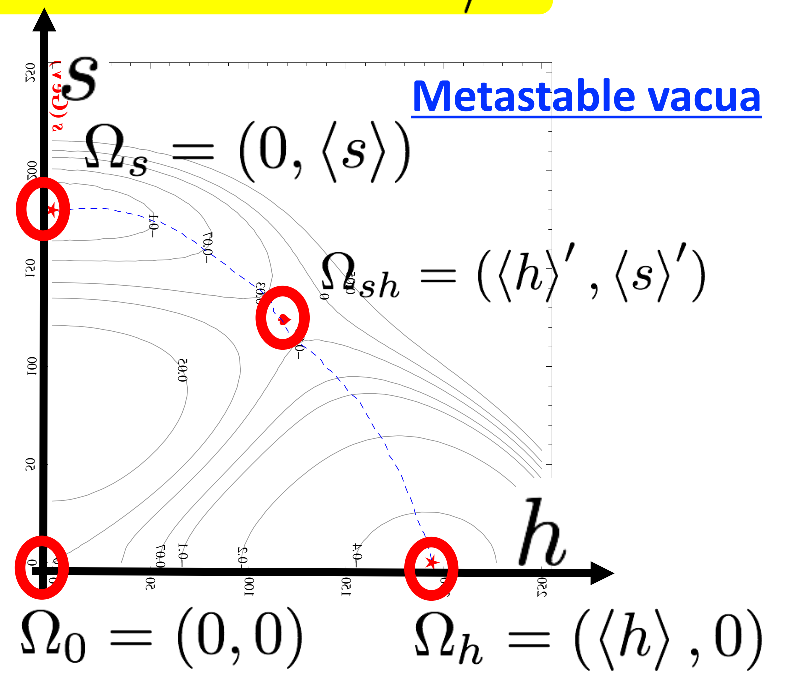

Allowed region of strongly 1stOPT via multi-step PT

arXiv:1706.09721 [hep-ph], Z. Kang, P. Ko, TM

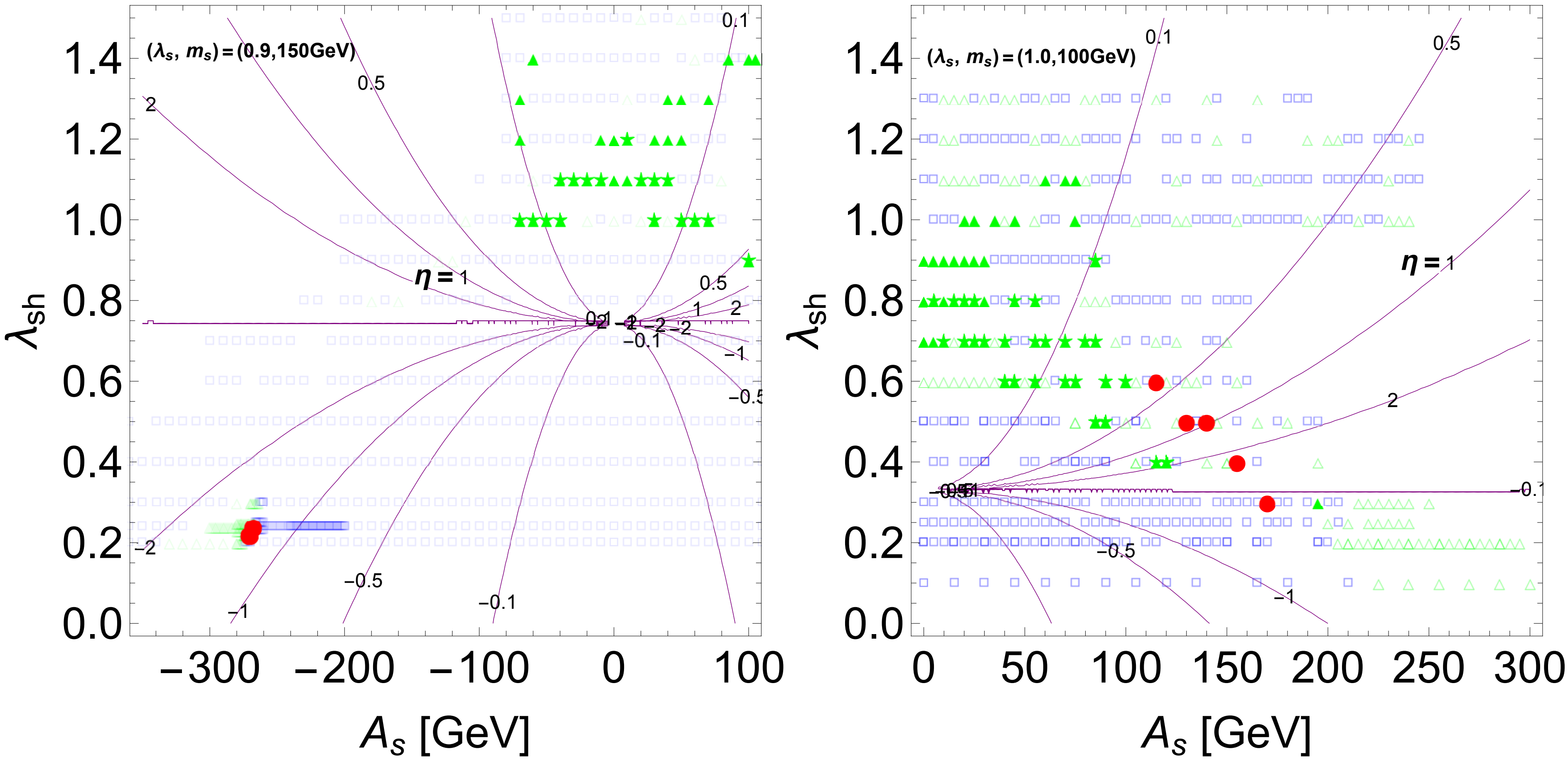

1st order EW phase transitions with multi-step

▲: Two-step PT (Z_2-like case), ★: Two-step PT (large A_s case), ●: Three-step PT

$\Omega_0 \xrightarrow{\text{2nd}} \Omega_s \xrightarrow{\text{1st}} \Omega_h$ $\Omega_0 \xrightarrow{\text{1st}} \Omega_s \xrightarrow{\text{1st}} \Omega_h$ $\Omega_0 \xrightarrow{\text{1st}} \Omega_s \xrightarrow{\text{2nd}} \Omega_{sh} \xrightarrow{\text{1st}} \Omega_h$

□: 2nd order EWPT (one-step)

Transition temperatures

arXiv:1706.09721 [hep-ph], Z. Kang, P. Ko, TM

Two step PT (Z_2-like case)

$$\Omega_0 \xrightarrow{\text{2nd}} \Omega_s \xrightarrow[T_*]{\text{1st}} \Omega_h$$

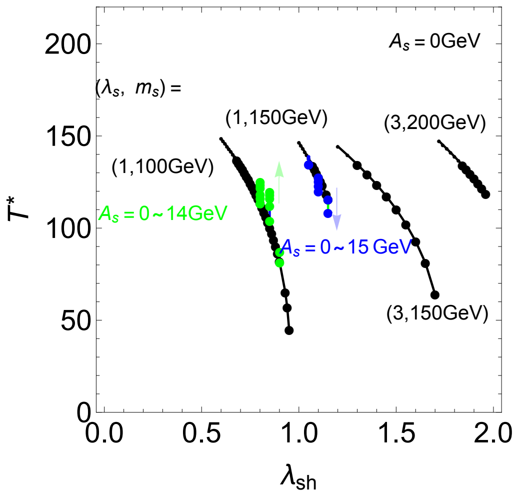

Two step PT (large A_s case)

$$\Omega_0 \xrightarrow[T_s^*]{\text{1st}} \Omega_s \xrightarrow[T_*]{\text{1st}} \Omega_h$$

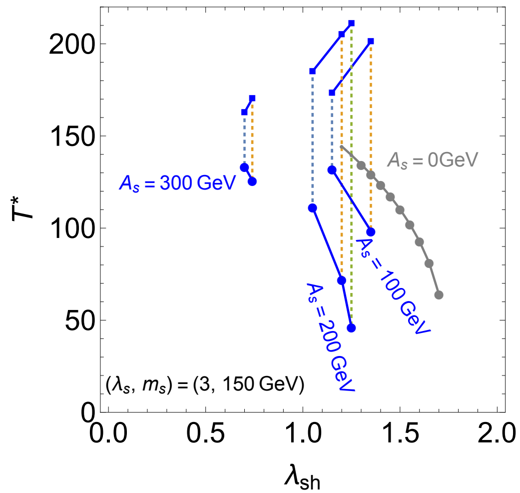

Three step PT

$$\Omega_0 \xrightarrow[T_s^*]{\text{1st}} \Omega_s \xrightarrow{\text{2nd}} \Omega_{sh} \xrightarrow[T_*]{\text{1st}} \Omega_h$$

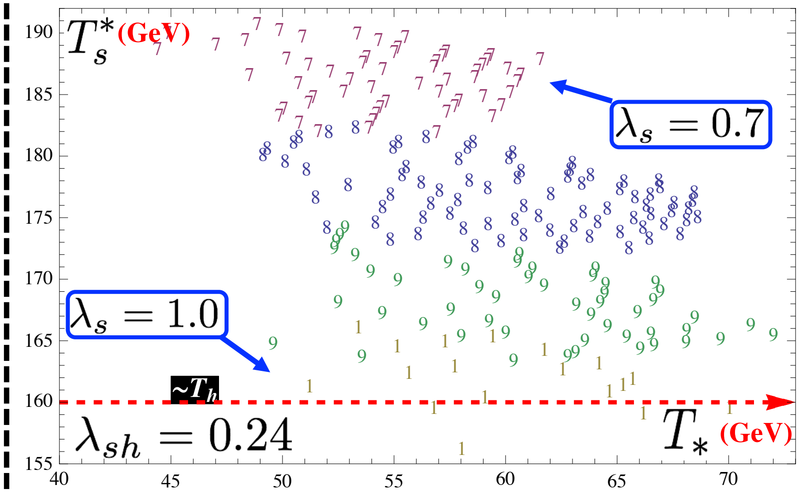

$$T_* \searrow \Longrightarrow \varphi_*/T_* \nearrow$$

Gravitational waves from 1stOPT

arXiv:1706.09721 [hep-ph], Z. Kang, P. Ko, TM

Two step PT (Z_2-like case)

$$\Omega_0 \xrightarrow{\text{2nd}} \Omega_s \underset{T_*}{\xrightarrow{\text{1st}}} \Omega_h$$

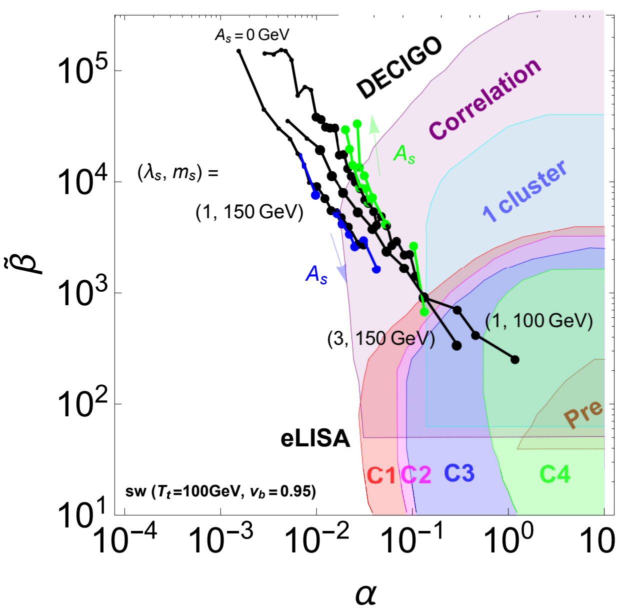

Two step PT (large A_s case)

$$\Omega_0 \underset{T_s^*}{\xrightarrow{\text{1st}}} \Omega_s \underset{T_*}{\xrightarrow{\text{1st}}} \Omega_h$$

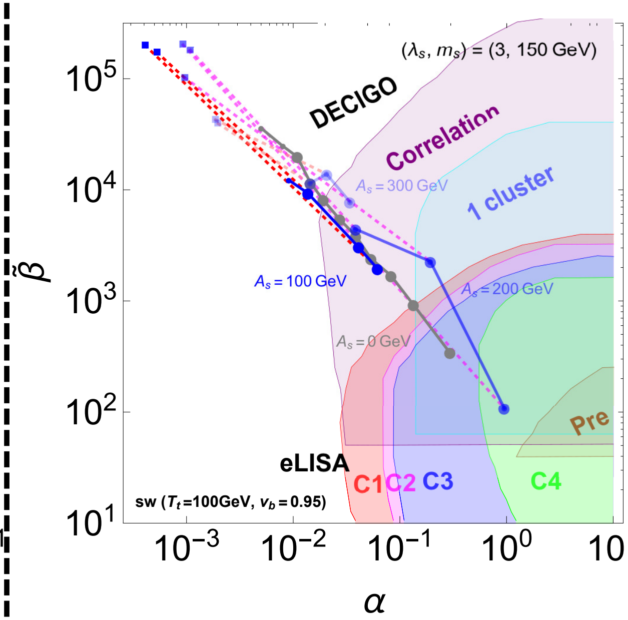

Three step PT

$$\Omega_0 \underset{T_s^*}{\xrightarrow{\text{1st}}} \Omega_s \xrightarrow{\text{2nd}} \Omega_{sh} \underset{T_*}{\xrightarrow{\text{1st}}} \Omega_h$$

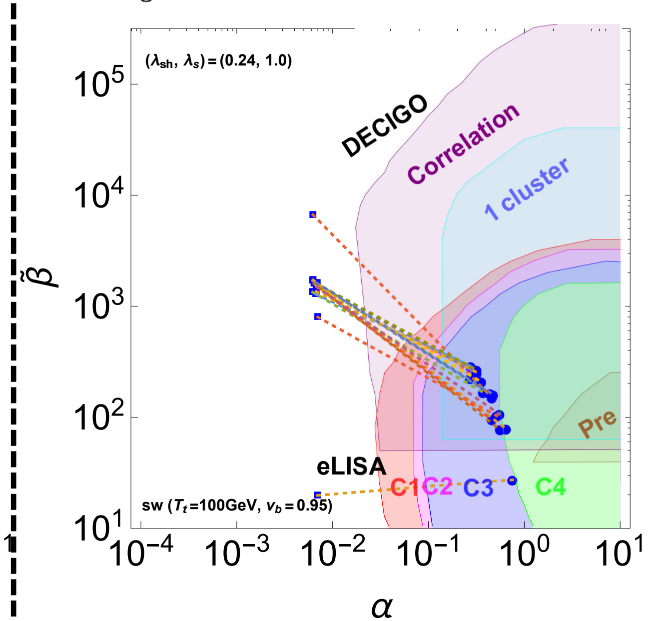

Sensitivities

- DECIGO [S.Kawamura, et al., Class. Quant. Grav. 28, 094011 (2011)]
- eLISA [C.Caprini *et al.*, arXiv:1512.06239 [astro-ph.CO]]

Conclusions

- We have not understood the shape of the Higgs potential.
- Basically, 1stOPT which is realized by models with extended Higgs sector can be tested at the colliders by measuring the Higgs cubic coupling.

- However, there is another case: "nightmare scenario", when we consider a scenario that the potential barrier is created by "the multi-step PT".

- In this talk, we have focused on a model with unbroken discrete symmetry.
- We have shown that, even if it is difficult to test at the colliders,
  - GW is significantly enhanced by the strongly 1stOPT
  - GW can be detected by future interferometers such as LISA/DECIGO

Back Up

Electroweak Baryogenesis

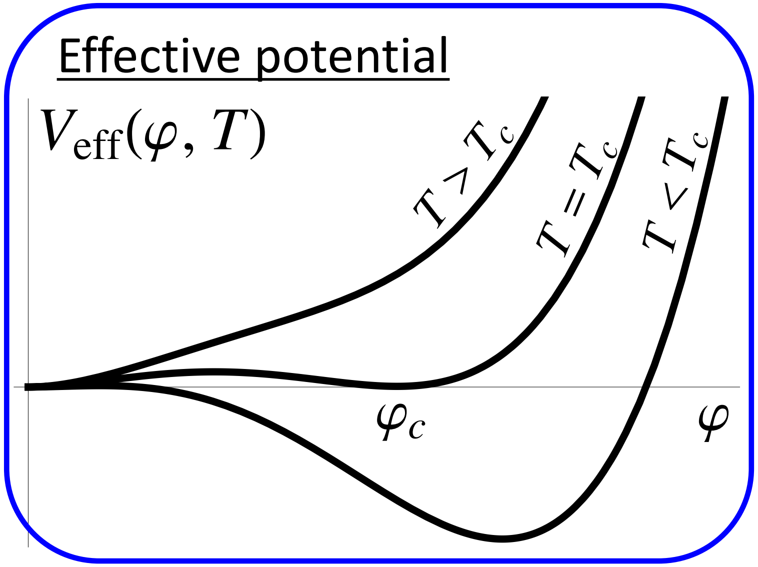

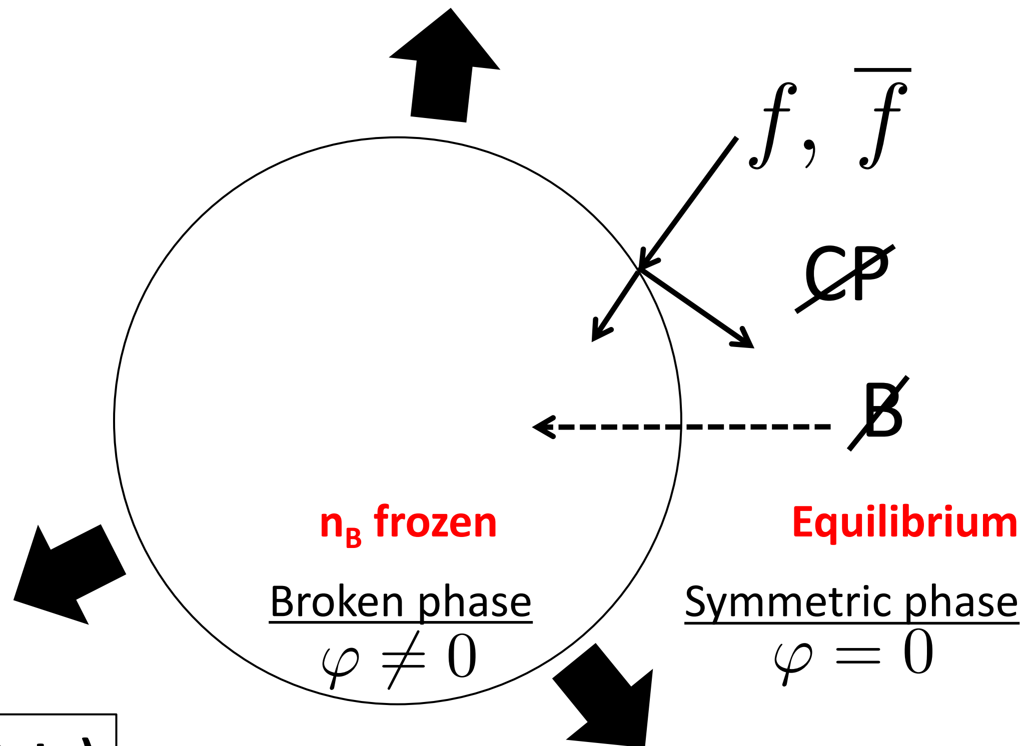

(Sphaleron Rate)<<(Expansion Rate)

Sphaleron decoupling condition is required to explain sufficient #B in broken phase.

$$\boxed{\varphi_c/T_c \gtrsim 1}$$

"Condition of strongly 1st order EWPT"

Triple Higgs boson coupling measurements

- HL-LHC (14TeV, 3000fb^{-1})

$\Delta\lambda_{hhh}/\lambda_{hhh}$~50%($gg \rightarrow hh$)

Snowmass Higgs working group,
arXiv:1310.8361 [hep-ex]

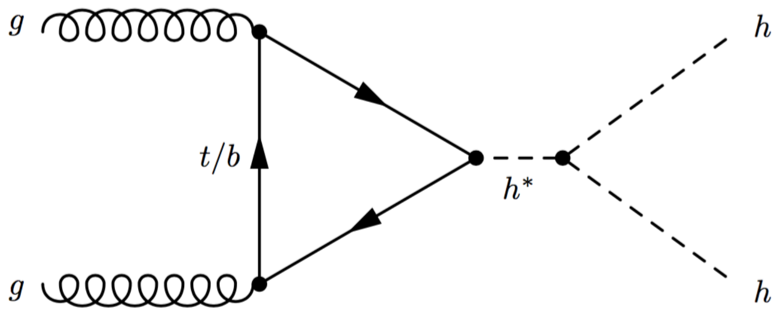

- ILC1000-up (500/1000GeV, 1600+2500fb^{-1})

$\Delta\lambda_{hhh}/\lambda_{hhh}$~10%($ee \rightarrow \nu\nu hh$)

K.Fujii *et al.*, arXiv:1506.05992 [hep-ex]

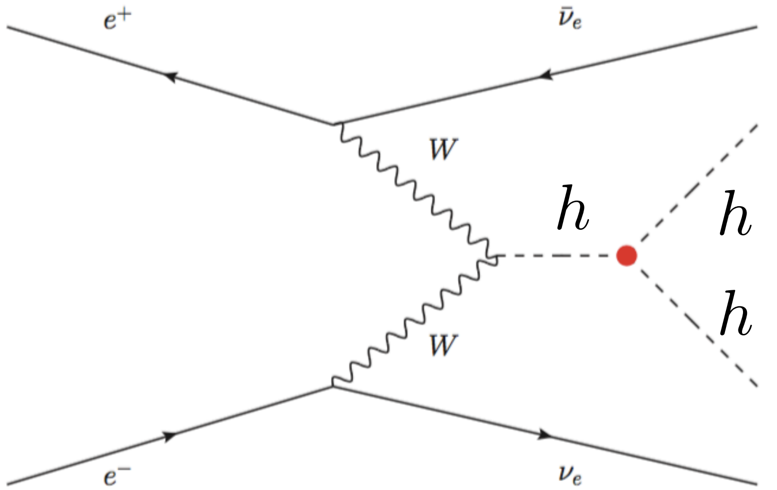

Theoretical constraints

- Perturbative unitarity: $|a_0(W_L^+W_L^- \to W_L^+W_L^-)| \leq 1$

$$m_h^2 \cos^2\theta + m_H^2 \sin^2\theta \leq \frac{4\pi\sqrt{2}}{3G_F} \approx (700\mathrm{GeV})^2$$

- Vacuum stability:

$$\lambda_\Phi(\mu) > 0, \qquad \lambda_S(\mu) > 0, \qquad 4\lambda_\Phi(\mu)\lambda_S(\mu) > \lambda_{\Phi S}^2(\mu)$$

- Landau pole:

$$|\lambda_{\Phi,S,\Phi S}(\Lambda_{\mathrm{LP}})| = 4\pi$$

- Oblique parameters (*S*, *T*, *U*):

$$\cos\theta \gtrsim 0.92 \quad \text{when } m_H \gtrsim 400\mathrm{GeV}\ (m_h \approx 125\mathrm{GeV})$$

S. Baek, P. Ko, W. I. Park and E. Senaha, JHEP 1211, 116 (2012)

Direct searches for the additional Higgs boson in the HSM at the LHC

Upper limit on the Higgs mixing angle $|\sin\theta|$

[Robens, Stefaniak (2016)]

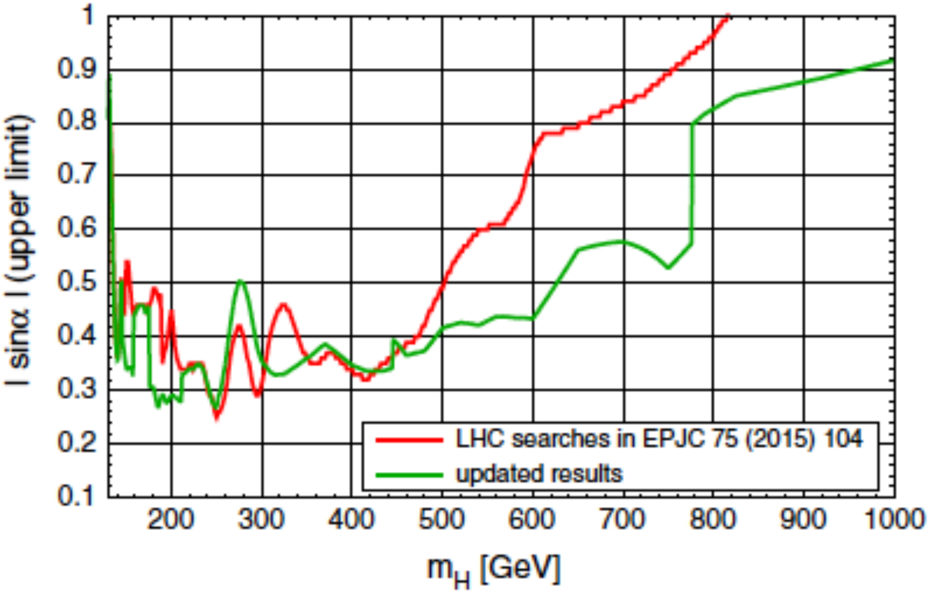

Range of m_H [GeV]	Search channel
130–145	$H \to ZZ \to 4l$
145–158	$H \to VV$ (V=W,Z)
158–163	SM comb.
163–170	$H \to WW$
170–176	SM comb.
176–211	$H \to VV$ (V=W,Z)
211–225	$H \to ZZ \to 4l$
225–445	$H \to VV$ (V=W,Z)

Constraints on the Higgs boson coupling $\kappa(= \cos\theta)$

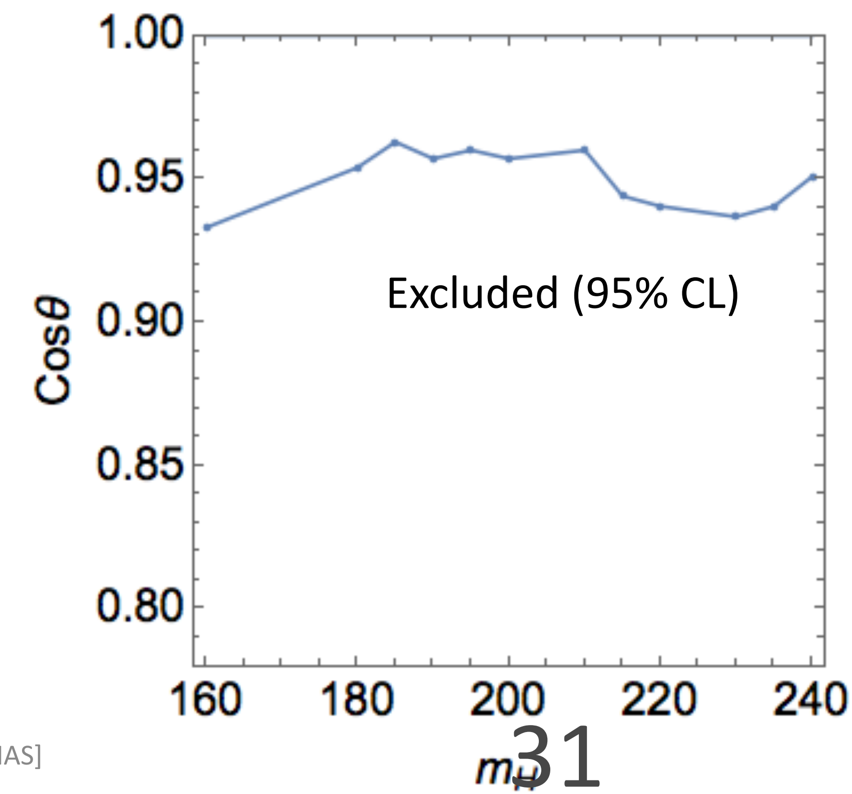

Multi-field analysis of EWPT

K. Funakubo, S. Tao and F. Toyoda, Prog. Theor. Phys. 114, 369 (2005) (NMSSM)
K. Fuyuto and E. Senaha, Phys. Rev. D 90, no. 1, 015015 (2014) (HSM)

- EWPT:

$$(\varphi_\Phi, \varphi_S)_{\rm SYM} \to (\varphi_\Phi, \varphi_S)_{\rm EW}$$ @T=T_c, $\varphi_c \equiv \varphi_\Phi(T_c)$

- Diverse patterns of the EWPT:

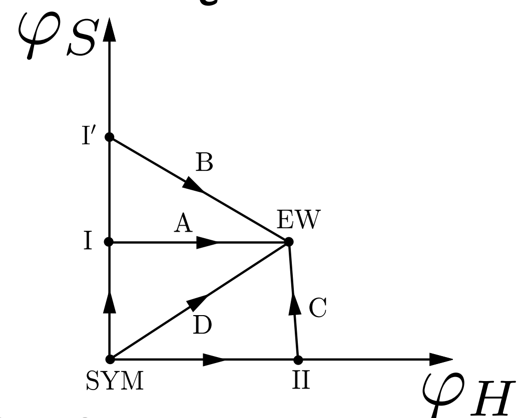

- EW phase needs to be the global min.:

$$V_{{\rm eff},T=0}({\rm EW\ phase}) < V_{{\rm eff},T=0}({\rm other\ phases})$$

- Public tool “CosmoTransition” (Python code) is used.

Dark Matter: Z_2-like case($A_s \to 0$)

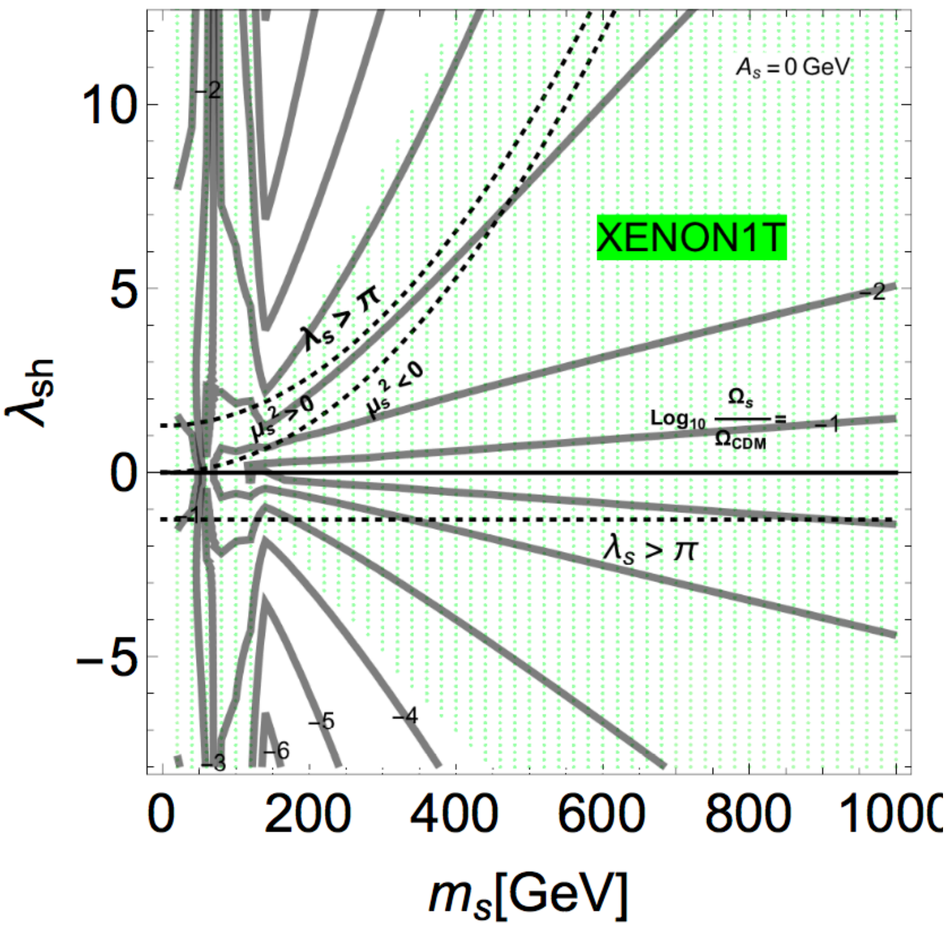

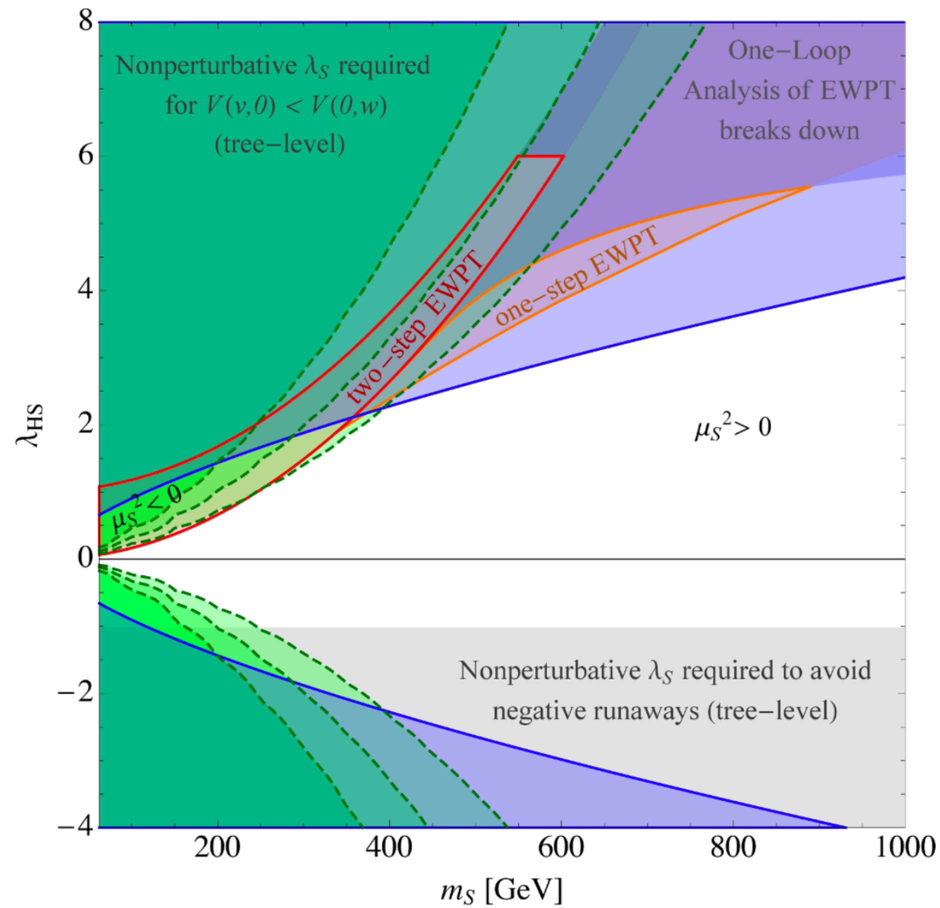

Curtin, Meade, Yu, 1409.0005

Dark Matter: finite A_s

100GeV

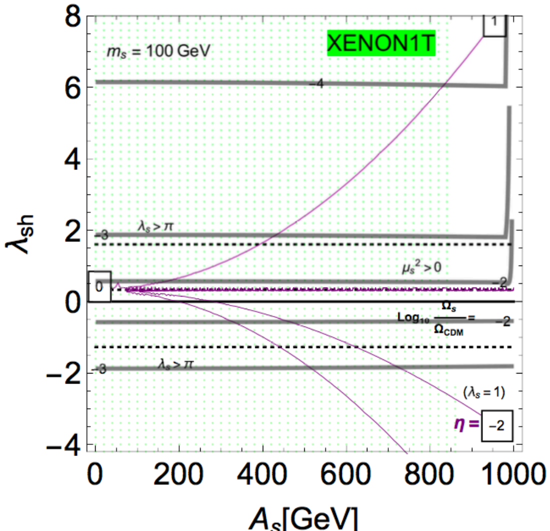

150GeV

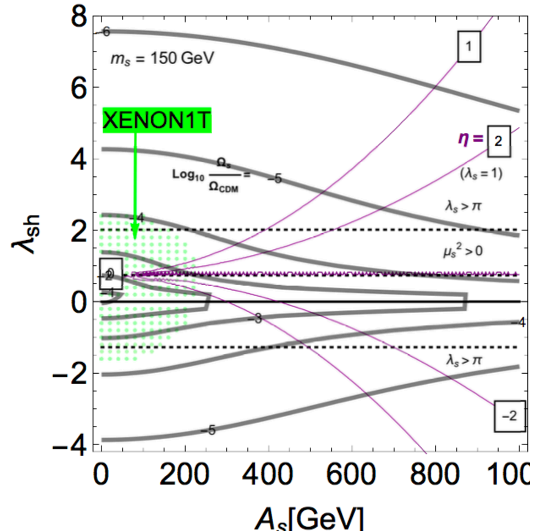

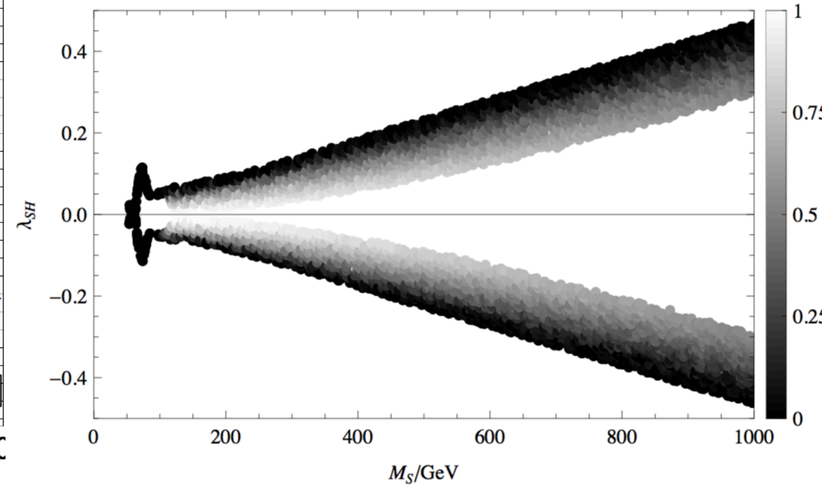

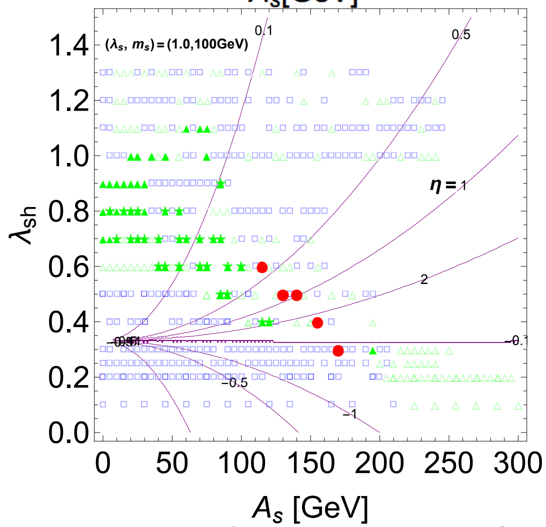

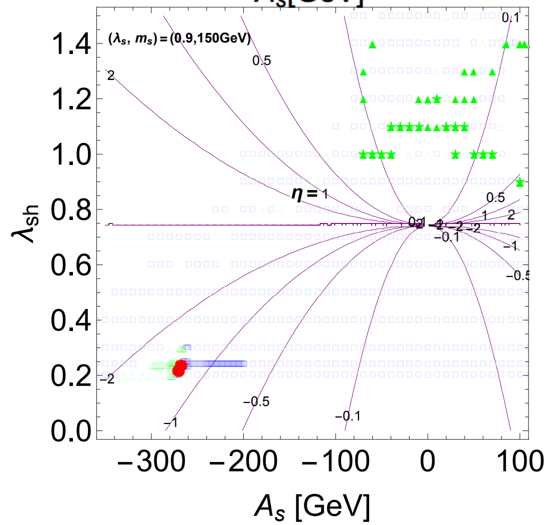

semi-annihilation is realized for small λ_{sh}

[Belanger, Kannike, Pukhovd, Raidal, 1211.1014]

However, the parameter regions which realize the strongly 1stOPT are not explained whole of the observed DM relic density.

Models of 1stOPT

<u>Higgs potential by high temperature approximation</u>

$$V_{\rm eff} = D(T^2 - T_0^2)\varphi^2 - (ET - e)\varphi^3 + \frac{\lambda(T)}{4}\varphi^4 \Rightarrow \boxed{\frac{\varphi_c}{T_c} = \frac{2E}{\lambda}\left(1 - \frac{e\lambda}{ET}\right)}$$

- *E* : thermal coupling (the non-decoupling effects due to the additional boson loop)
- −*e* : non-thermal coupling (the field mixing of the Higgs boson with additional scalar fields)

J. Kehayias and S. Profumo, JCAP**1003**, 003 (2010)

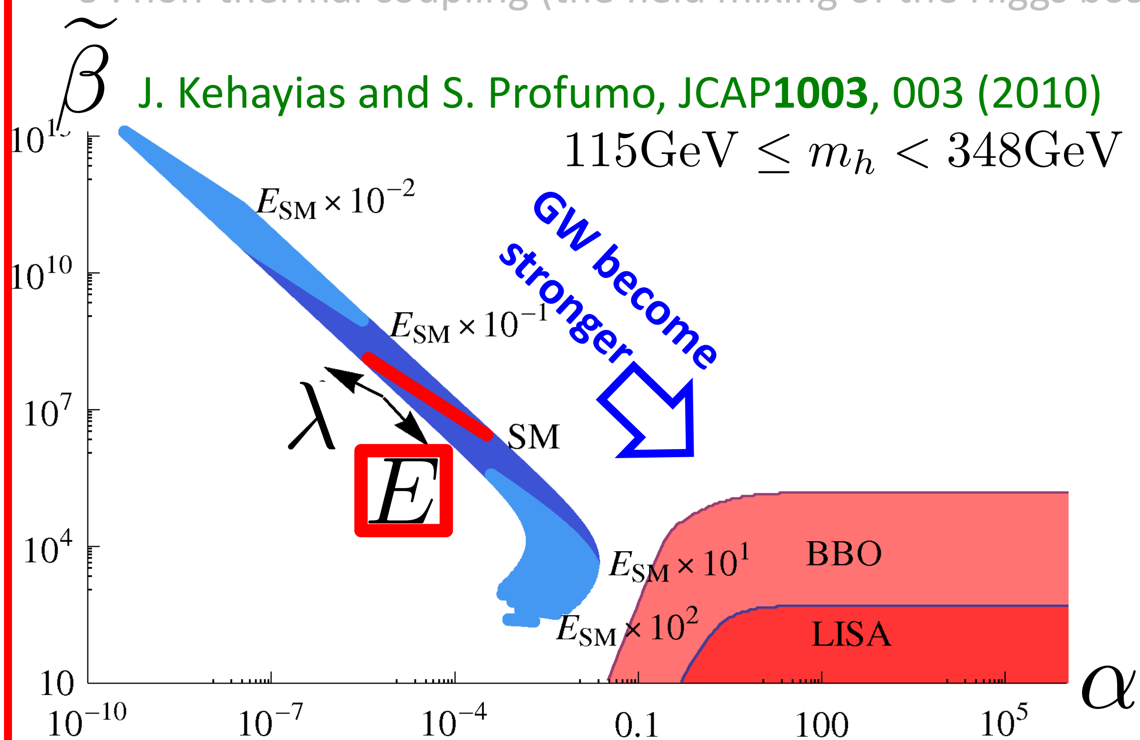

As the simplest model, we have investigated **the O(N) model**.

Kakizaki, Kanemura, TM, PRD **92**, 115007 (2015);
Hashino, Kakizaki, Kanemura, TM, PRD **94**, 015005 (2016)

Models of 1stOPT

<u>Higgs potential by high temperature approximation</u>

$$V_{\text{eff}} = D(T^2 - T_0^2)\varphi^2 - (ET - e)\varphi^3 + \frac{\lambda(T)}{4}\varphi^4 \Rightarrow \boxed{\frac{\varphi_c}{T_c} = \frac{2E}{\lambda}\left(1 - \frac{e\lambda}{ET}\right)}$$

- E : thermal coupling (the non-decoupling effects due to the additional boson loop)
- $-e$: non-thermal coupling (the field mixing of the Higgs boson with additional scalar fields)

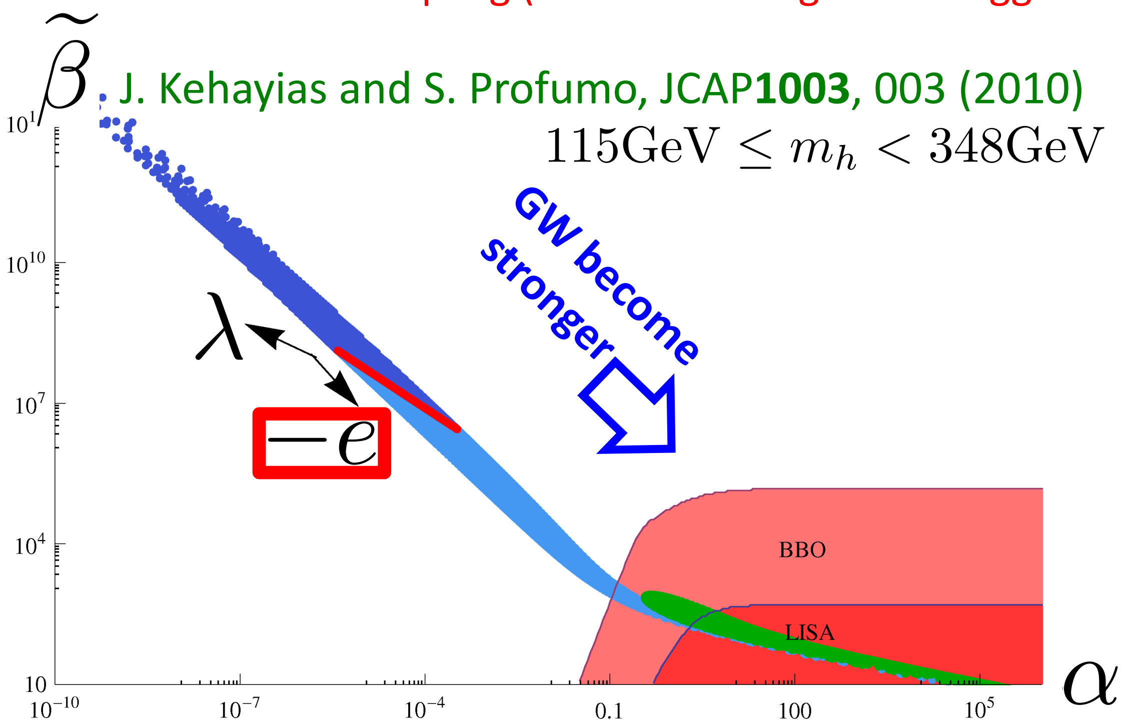

As the simplest model, we have investigated **Z_3 symmetric model**.

arXiv:1706.09721 [hep-ph], Kang, Ko, TM

Models of 1stOPT

Higgs potential by high temperature approximation

$$V_{\text{eff}} = D(T^2 - T_0^2)\varphi^2 - (ET - e)\varphi^3 + \frac{\lambda(T)}{4}\varphi^4 \quad \Rightarrow \quad \boxed{\frac{\varphi_c}{T_c} = \frac{2E}{\lambda}\left(1 - \frac{e\lambda}{ET}\right)}$$

- E : thermal coupling (the non-decoupling effects due to the additional boson loop)
- $-e$: non-thermal coupling (the field mixing of the Higgs boson with additional scalar fields)

``O(N) model''

N iso-singlet fields with O(N) sym. $\vec{S} = (S_1, S_2, \cdots, S_N)^T$

M.Kakizaki, S.Kanemura, T.Matsui, Phys. Rev. D **92**, no. 11, 115007 (2015)

$$V_0(\Phi, \vec{S}) = -\mu^2|\Phi|^2 + \frac{\mu_S^2}{2}|\vec{S}|^2 + \frac{\lambda}{4}|\Phi|^4 + \frac{\lambda_S}{4}|\vec{S}|^4 + \frac{\lambda_{\Phi S}}{2}|\Phi|^2|\vec{S}|^2$$

- O(N) is not broken → Common mass of S$_i$: $m_S^2 = \mu_S^2 + \frac{\lambda_{\Phi S}}{2}v^2$
- Model parameters: (N, m_S, μ_S)
- 1stOPT: $\boxed{E = \frac{1}{12\pi v^3}\left\{6m_{W^\pm}^3 + 3m_Z^3 + N\, m_S^3\left(1 - \frac{\mu_S^2}{m_S^2}\right)^3\left(1 + \frac{3}{2}\frac{\mu_S^2}{m_S^2}\right)\right\}}$

$V_{\rm eff}(\varphi, T) \rightarrow \boxed{\Delta\lambda_{hhh}}$

$\varphi_c/T_c \nearrow \Rightarrow \Delta\lambda_{hhh} \nearrow$

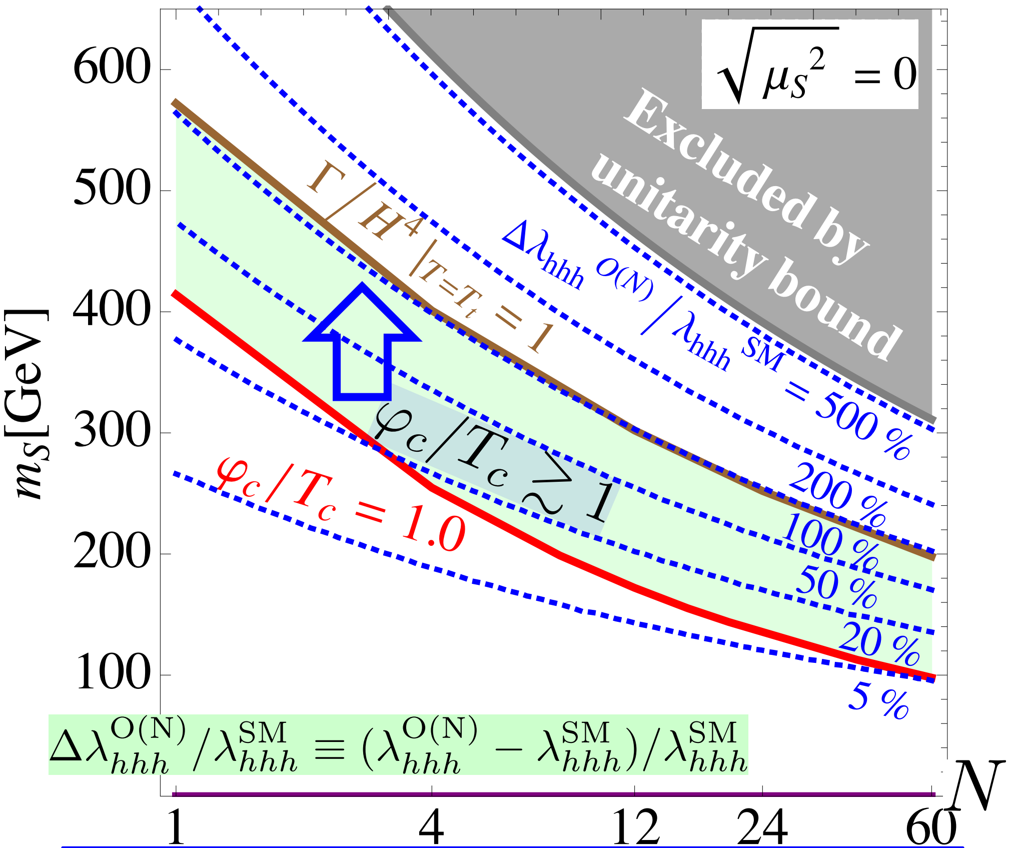

$$\Delta\lambda_{hhh}^{\rm O(N)}/\lambda_{hhh}^{\rm SM} \equiv (\lambda_{hhh}^{\rm O(N)} - \lambda_{hhh}^{\rm SM})/\lambda_{hhh}^{\rm SM}$$

$$\lambda_{hhh}^{\rm O(N)} \equiv \frac{3m_h^2}{v}\left\{1 - \frac{m_t^4}{\pi^2 m_h^2 v^2} + \underline{\frac{N m_S^4}{12\pi^2 m_h^2 v^2}\left(1 - \frac{\mu_S^2}{m_S^2}\right)^3}\right\}$$

M.Kakizaki, S.Kanemura, T.Matsui, Phys. Rev. D **92**, no. 11, 115007 (2015)

$\varphi_c/T_c \nearrow \Rightarrow \Delta\lambda_{hhh} \nearrow$

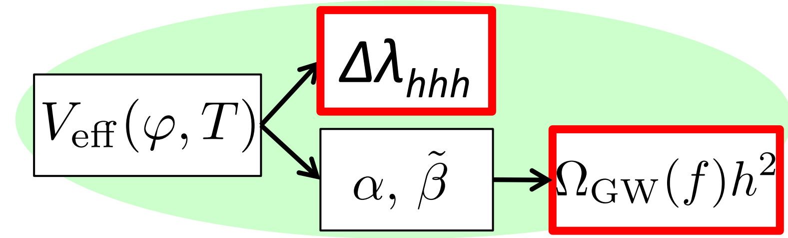

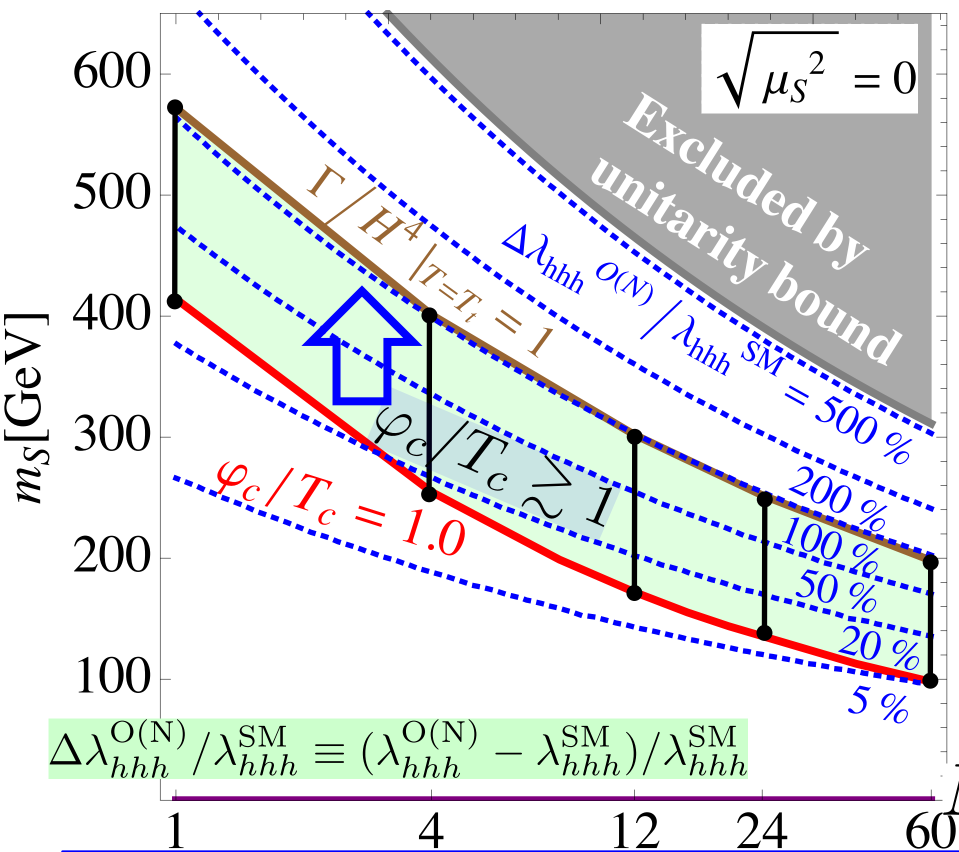

$$\lambda^{\rm O(N)}_{hhh} \equiv \frac{3m_h^2}{v}\left\{1 - \frac{m_t^4}{\pi^2 m_h^2 v^2} + \frac{N m_S^4}{12\pi^2 m_h^2 v^2}\left(1 - \frac{\mu_S^2}{m_S^2}\right)^3\right\}$$

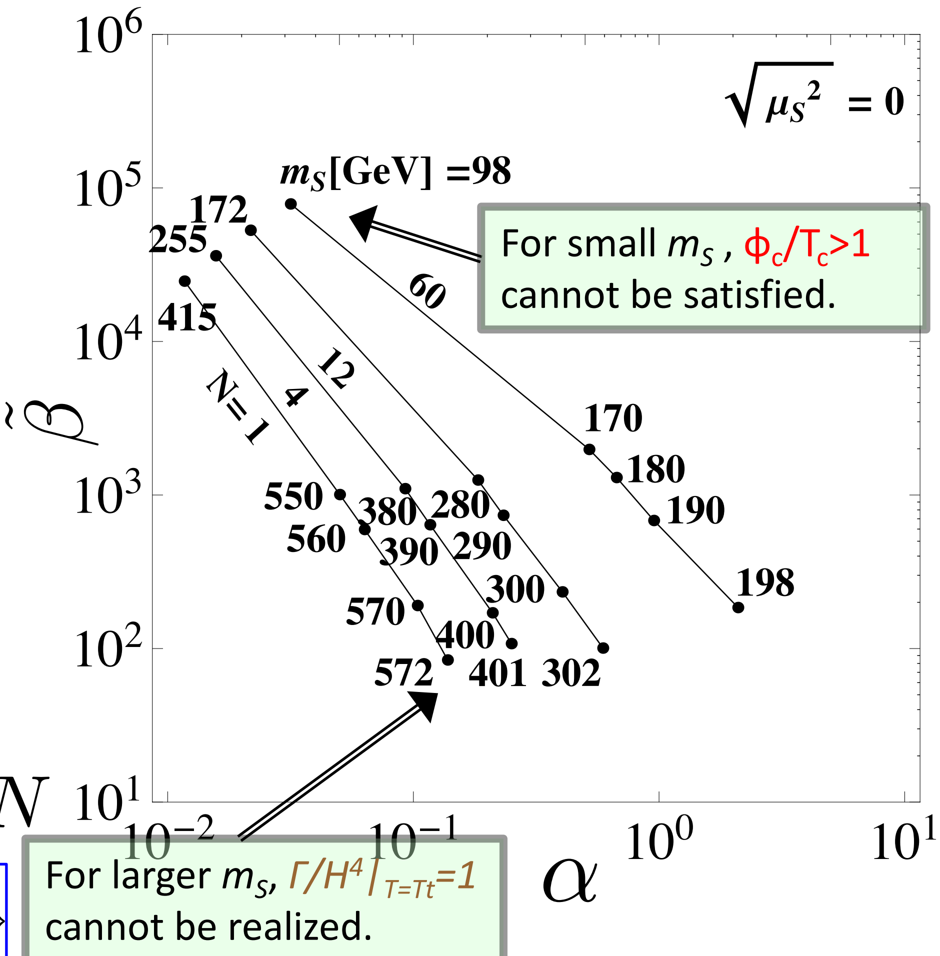

M.Kakizaki, S.Kanemura, T.Matsui, Phys. Rev. D **92**, no. 11, 115007 (2015)

Higgs singlet model

K. Hashino, M. Kakizaki, S. Kanemura, T. Matsui, P. Ko, PLB **766**, 49 (2017)

$$V_0 = -\mu_\Phi^2|\Phi|^2 + \lambda_\Phi|\Phi|^4 + \mu_{\Phi S}|\Phi|^2 S + \frac{\lambda_{\Phi S}}{2}|\Phi|^2 S^2 + \mu_S^3 S + \frac{m_S^2}{2}S^2 + \frac{\mu_S'}{3}S^3 + \frac{\lambda_S}{4}S^4$$

S: a real singlet

$$\frac{\Delta\lambda_{hhh}}{\lambda_{hhh}} \equiv \frac{\lambda_{hhh} - \lambda_{hhh}^{\rm SM}}{\lambda_{hhh}^{\rm SM}}$$

$$\lambda_{hhh}^{\rm HSM,tree} = 6\left(\lambda_\Phi v_\Phi c_\theta^3 + \frac{\mu_{\Phi S}}{2}s_\theta c_\theta^2 + \frac{\lambda_{\Phi S}}{2}s_\theta c_\theta(v_\Phi s_\theta + v_S c_\theta) + \left(\frac{\mu_S'}{3} + \lambda_S v_S\right)s_\theta^3\right)$$

$$\kappa_i \equiv g_{hii}/g_{hii}^{\rm SM} \qquad \kappa \equiv \kappa_V = \kappa_F = \cos\theta$$

(Universality)

θ: mixing angle

$$\frac{\varphi_c}{T_c} = \frac{2E}{\lambda}\left(1 - \frac{e\lambda}{ET}\right)$$

$$e = \left(\mu_{\Phi S}\cos^2\alpha + \frac{\mu_S'}{3}\sin^2\alpha\right)\sin\alpha$$ <0

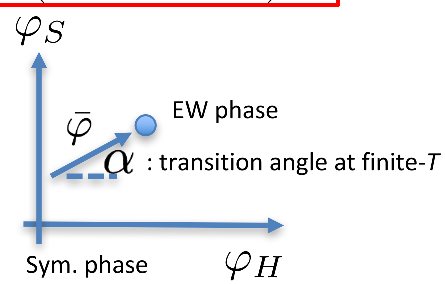

v_Φ [GeV]	v_S [GeV]	m_h [GeV]	$\mu_{\Phi S}$ [GeV]	μ_S' [GeV]	μ_S [GeV]	m_H [GeV]	θ [degrees]
246.2	90	125.5	−80	−30	0	[160, 240]	[−15, −35]

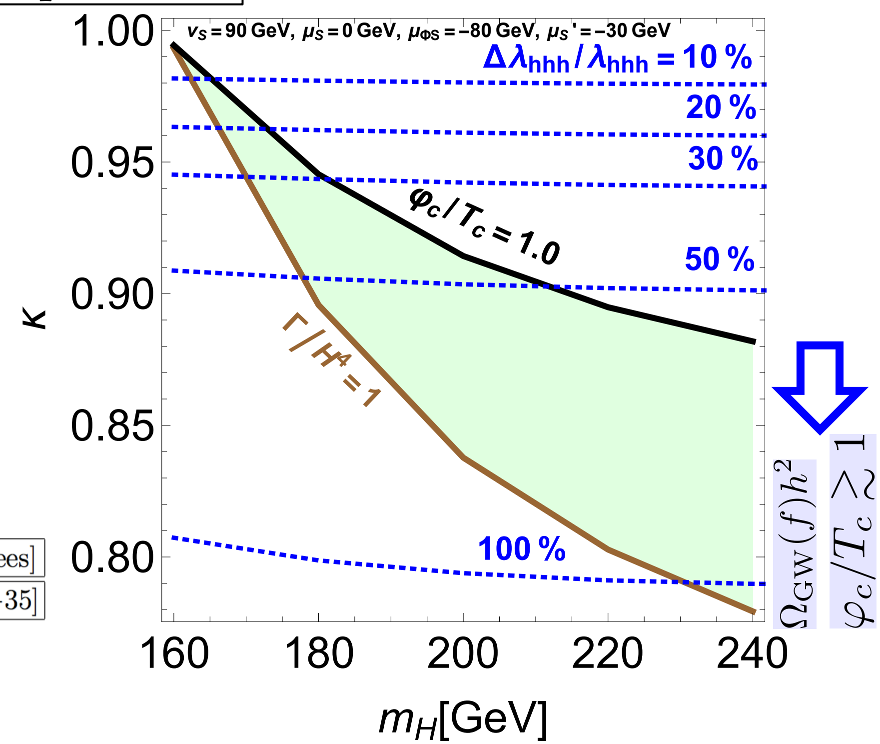

Higgs singlet model

K. Hashino, M. Kakizaki, S. Kanemura, T. Matsui, P. Ko, PLB **766**, 49 (2017)

$$V_0 = -\mu_\Phi^2|\Phi|^2 + \lambda_\Phi|\Phi|^4 + \mu_{\Phi S}|\Phi|^2 S + \frac{\lambda_{\Phi S}}{2}|\Phi|^2 S^2 + \mu_S^3 S + \frac{m_S^2}{2} S^2 + \frac{\mu'_S}{3} S^3 + \frac{\lambda_S}{4} S^4$$

S: a real singlet

$$\frac{\Delta\lambda_{hhh}}{\lambda_{hhh}} \equiv \frac{\lambda_{hhh} - \lambda_{hhh}^{\rm SM}}{\lambda_{hhh}^{\rm SM}}$$

$$\lambda_{hhh}^{\rm HSM,tree} = 6\left(\lambda_\Phi v_\Phi c_\theta^3 + \frac{\mu_{\Phi S}}{2} s_\theta c_\theta^2 + \frac{\lambda_{\Phi S}}{2} s_\theta c_\theta (v_\Phi s_\theta + v_S c_\theta) + \left(\frac{\mu'_S}{3} + \lambda_S v_S\right) s_\theta^3\right)$$

$$\kappa_i \equiv g_{hii}/g_{hii}^{\rm SM} \qquad \kappa \equiv \kappa_V = \kappa_F = \cos\theta$$

(Universality)

θ: mixing angle

$$\frac{\varphi_c}{T_c} = \frac{2E}{\lambda}\left(1 - \frac{e\lambda}{ET}\right)$$

$$e = \left(\mu_{\Phi S}\cos^2\alpha + \frac{\mu'_S}{3}\sin^2\alpha\right)\sin\alpha$$ <0

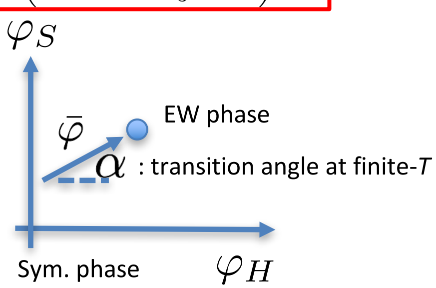

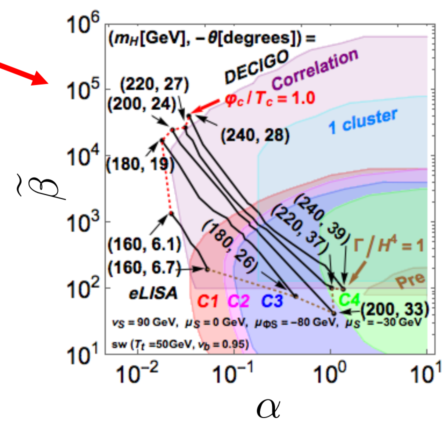

v_Φ [GeV]	v_S [GeV]	m_h [GeV]	$\mu_{\Phi S}$ [GeV]	μ'_S [GeV]	μ_S [GeV]	m_H [GeV]	θ [degrees]
246.2	90	125.5	−80	−30	0	[160, 240]	[−15, −35]

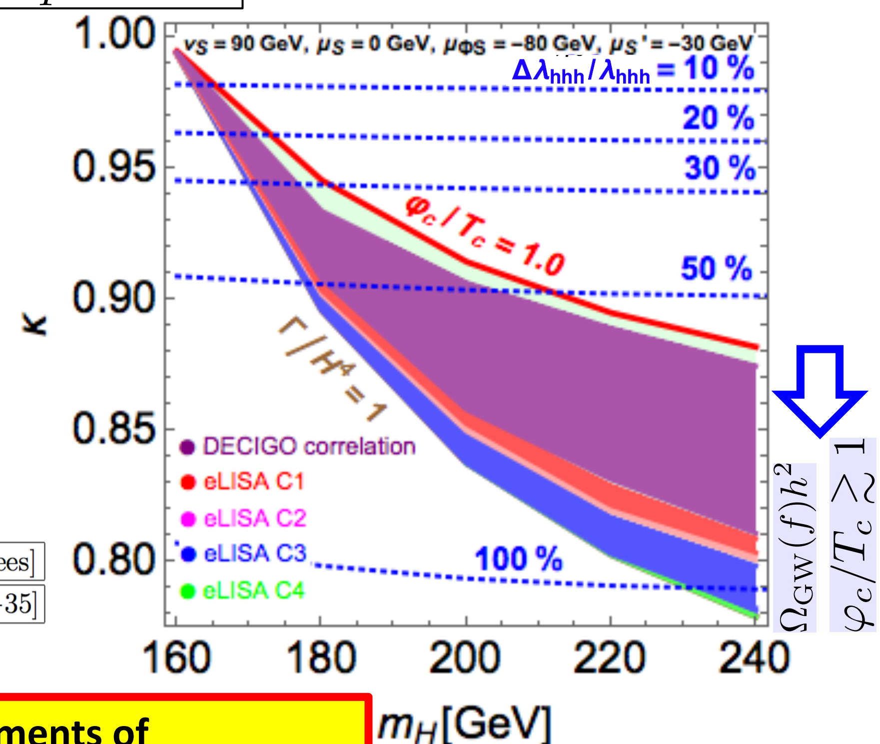

The synergy between the precision measurements of various Higgs boson couplings and GWs at future experiments is important!

Gravitational wave observations

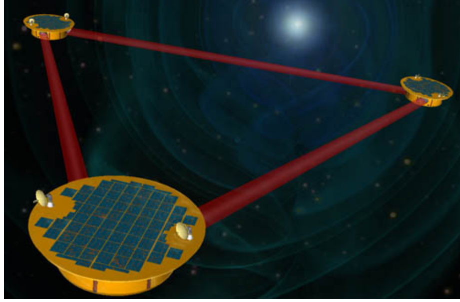

eLISA design decided

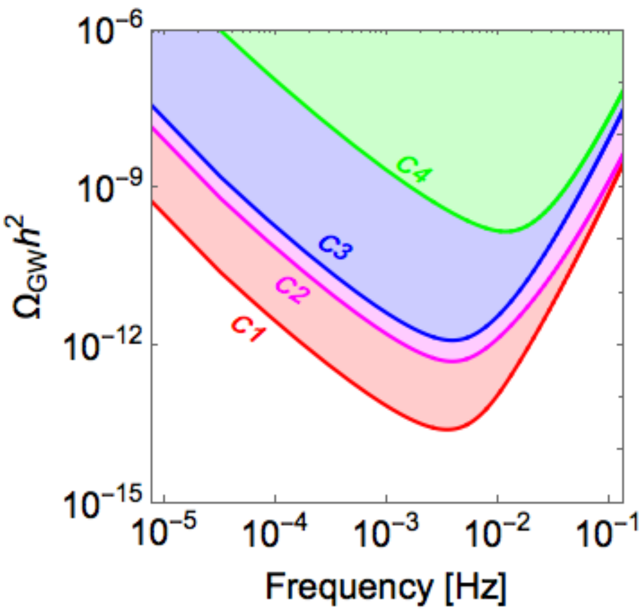

Properties of the representative eLISA configurations

Name	C1	C2	C3	C4
Full name	N2A5M5L6	N2A1M5L6	N2A2M5L4	N1A1M2L4
# links	6	6	4	4
Arm length [km]	5M	1M	2M	1M
Duration [years]	5	5	5	2
Noise level	N2	N2	N2	N1

eLISA cosmology WG report, arXiv:1512.06239 [JCAP(2016)]

C1 : old LISA configuration

- **Number of laser links : 6**, corresponding to **3** interferometer arms
  → Determined at eLISA symposium (Sept. 2016, U. of Zurich) http://www.physik.uzh.ch/events/lisa2016
- **Arm length : 2 - 5** million km
- **Duration : 3 - 10** years data taking

} Extra budget was estimated

- **Noise level** : **N2** (LISA pathfinder expected) is 10 times larger than N1 (LISA pathfinder required)
  → Determined by receiving the pathfinder result [PRL**116**, 231101 (2016)]

ESA approval : **June, 2017**
Launch : **2034**

Prospects for LIGO/Virgo

- LIGO 1st RUN (2015/09/12-2016/01/19)
- LIGO 2nd RUN (from the fall 2016)
  - 15-25% improvement in sensitivity performance over 1st RUN
  - The event rate will be increased by 1.5-2 times

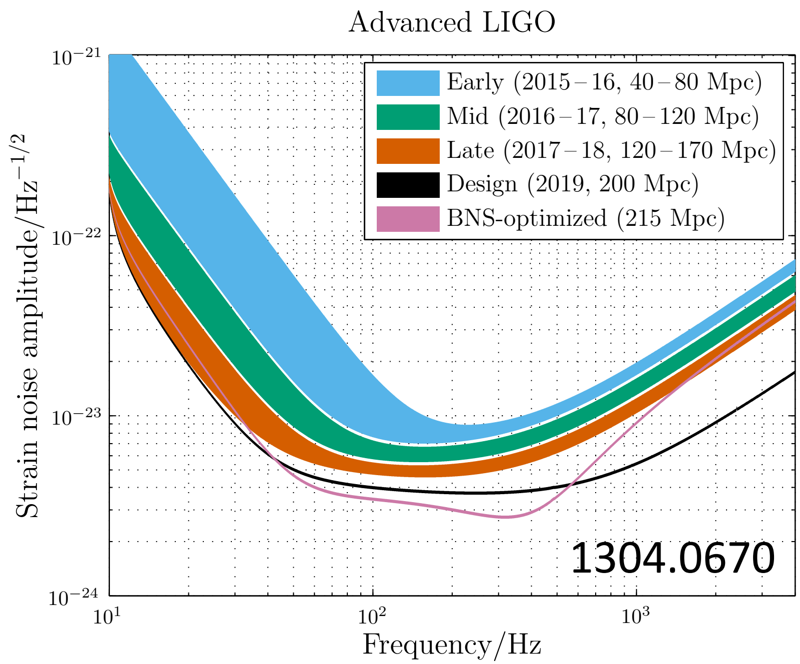

Observing run	Epoch	Duration (months)	aLIGO sensitivity	AdVirgo sensitivity
O1	2015–2016	4	Early	—
O2	2016–2017	6	Mid	Early
O3	2017–2018	9	Late	Mid
O4	2019	12	Design	Late
O5	2020+	–	Design	Design

1602.03847

Pulsar Timing Array

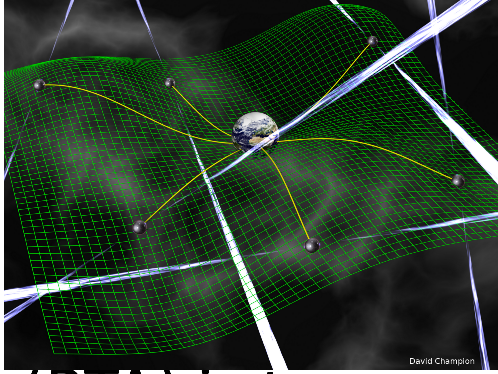

- The main idea behind pulsar timing array (PTA) is to use ultra-stable millisecond pulsars as beacons for detecting GW in the nano-Hz range ($10^{-9} - 10^{-7}$ Hz).
- Pulsars are neutron stars with rapid rotation and strong magnetic field. Period from few seconds to few milliseconds.

Pulsar Timing Array

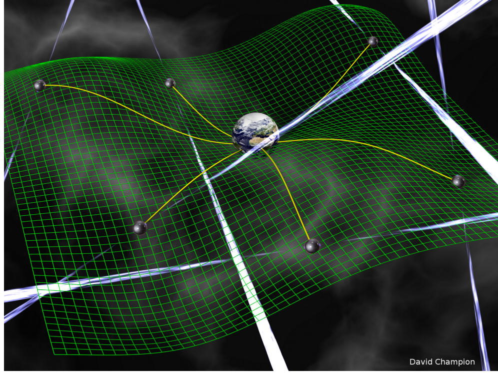

- Current limit: $\Omega_{GW}h^2 >\sim 10^{-9}$

  EPTA Collaboration [Mon. Not. Roy. Astron. Soc. **453**, no. 3, 2576 (2015) [arXiv:1504.03692]]

  NANOGrav Collaboration [Astrophys. J. **821**, no. 1, 13 (2016) [arXiv:1508.03024]]

- **International Pulsar Timing Array** (IPTA): combined three PTAs [PPTA (Australian), EPTA (European)*, NanoGrav (North American)]. *EPTA consists of 5 radio telescopes

  1st data release Mon. Not. Roy. Astron. Soc. **458**, 1267 (2016) [arXiv:1602.03640]

  Expected limit: $\Omega_{GW}h^2 >\sim 10^{-12}$ Publ. Astron. Soc. Austral. **30**, 17 (2013) [arXiv:1210.6130]

- **Square Kilometer Array** (SKA)

  : The next great advancement in radio astronomy

  Expected limit: $\Omega_{GW}h^2 >\sim 10^{-15}$ https://www.skatelescope.org

Gravitational wave from 1^{st} order phase transition

Estimation of the relic abundance

M. Kamionkowski, PRD**49**, 2837 (1994)

- Wave eq. from Einstein eq. in weak field approximation

$$-\Box\left(h_{\mu\nu} - \frac{1}{2}\eta_{\mu\nu}h^{\alpha}{}_{\alpha}\right) = 16\pi G T_{\mu\nu}$$

$$\begin{cases} T^0_0 = \rho_{\rm kin} + \cdots \\ \dfrac{d}{dt} \simeq \beta \end{cases}$$

- Stochastic backgrounds of GWs

$$\rho_{\rm GW} = \frac{1}{32\pi G} < \dot{h}_{\alpha\beta}\dot{h}^{\alpha\beta} > \sim \underline{8\pi G \rho^2_{\rm kin}/\beta^2}$$

$$\underline{\rho_{\rm tot}(= \underbrace{\rho_{\rm vac}}_{(=\epsilon)} + \rho_{\rm rad}) = \frac{3H^2}{8\pi G}} \qquad \alpha = \frac{\rho_{\rm vac}}{\rho_{\rm rad}} \qquad \kappa = \frac{\rho_{\rm kin}}{\rho_{\rm vac}}$$

Efficiency factor

$$\Omega_{\rm GW} = \frac{\rho_{GW}}{\rho_{\rm tot}} \simeq \underbrace{\left(\frac{H}{\beta}\right)^2}_{= \widetilde{\beta}^{-2} \sim (H\langle R\rangle)^2} \left(\frac{\kappa\alpha}{1+\alpha}\right)^2$$

Phase transition - Bubble configuration

Model parameters

Input

$V_{\text{eff}}(\varphi, T)$ $\xrightarrow{\Gamma(T)}$

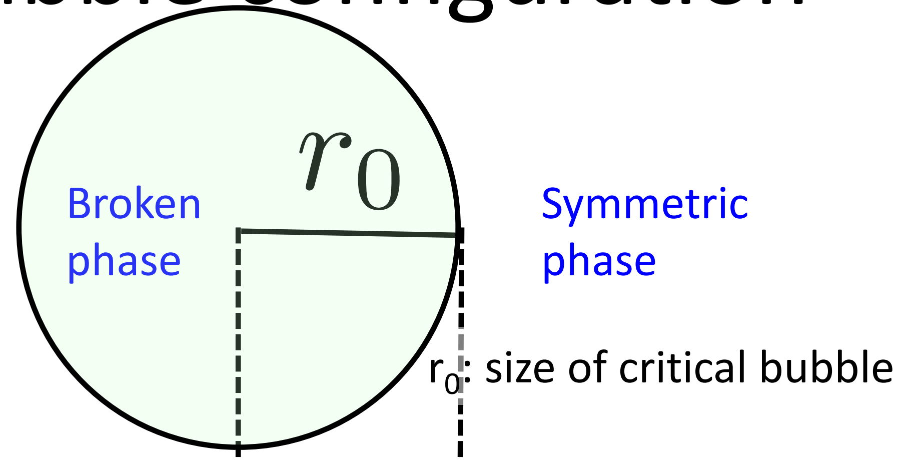

Potential:

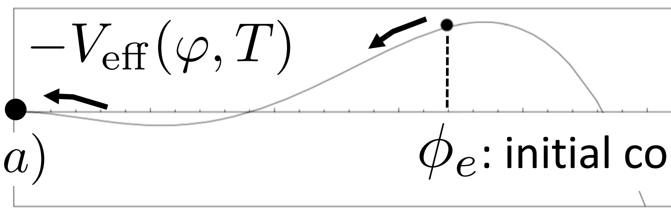

Eq. of motion: $\frac{d^2\varphi}{dr^2} + \frac{2}{r}\frac{d\varphi}{dr} - \frac{dV_{\text{eff}}}{d\varphi} = 0 \rightarrow \boxed{\varphi(r)}$

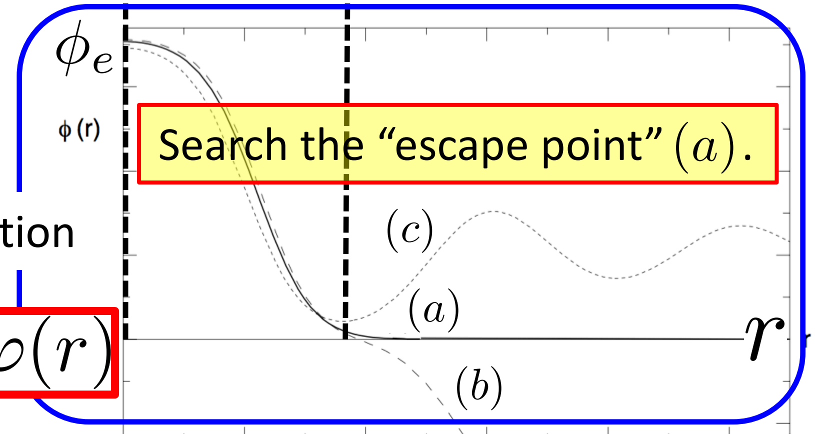

$\boxed{\varphi(r)}$ $\xrightarrow{\text{each}\,T}$

Bubble nucleation rate: $\Gamma(T) \simeq T^4 e^{-\frac{S_3(T)}{T}}$

3-dim. Euclidean action: $S_3(T) = \int dr^3 \left\{ \frac{1}{2}\left(\vec{\nabla}\varphi\right)^2 + V_{\text{eff}}(\varphi, T) \right\}$

Phase transition - Transition temperature

Model parameters

Input

$$V_{\text{eff}}(\varphi, T) \xrightarrow{\Gamma(T)}$$

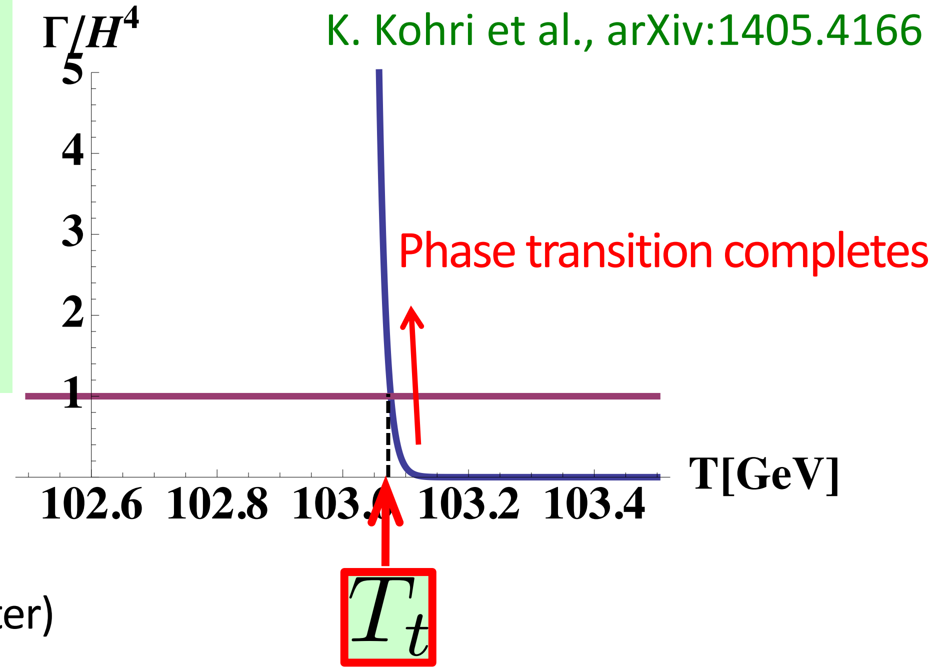

$$\boxed{\left.\frac{\Gamma}{H^4}\right|_{T=T_t} \simeq 1}$$ (H: Hubble parameter)

→ Definition of phase transition temperature T_t

Bubble nucleation rate: $\Gamma(T) \simeq T^4 e^{-\frac{S_3(T)}{T}}$

3-dim. Euclidean action: $S_3(T) = \int dr^3 \left\{ \frac{1}{2}\left(\vec{\nabla}\varphi\right)^2 + V_{\text{eff}}(\varphi, T) \right\}$

GWs from 1stOPT

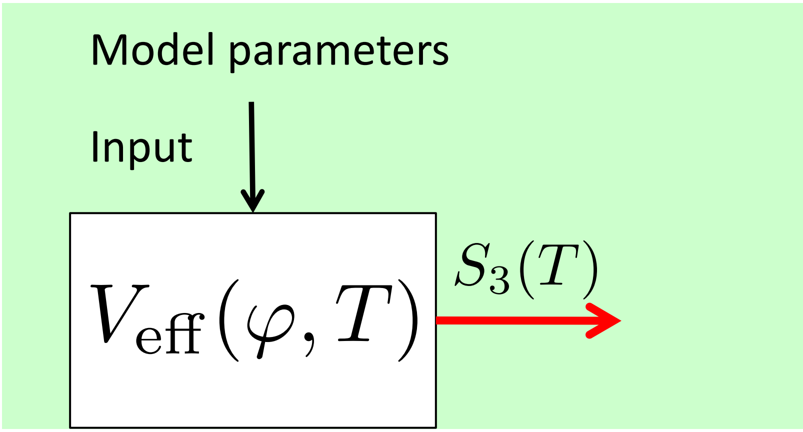

Definition of phase transition temperature T_t

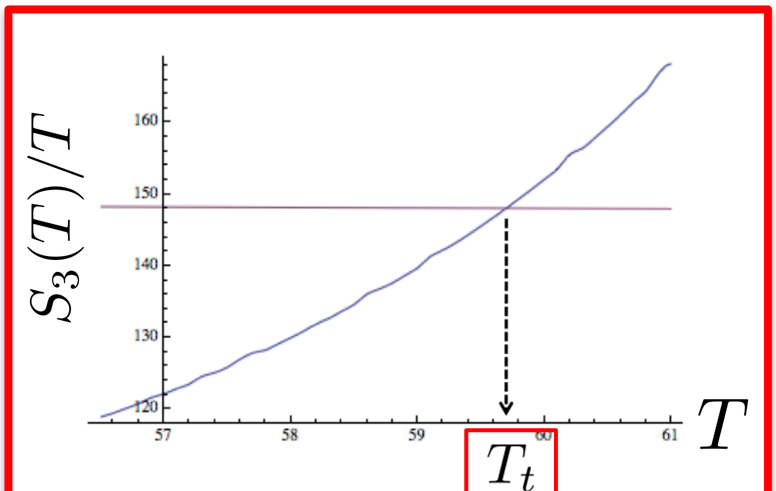

$$\left.\frac{\Gamma}{H^4}\right|_{T=T_t} \simeq 1 \quad \leftrightarrows \quad \left.\frac{S_3(T)}{T}\right|_{T=T_t} \simeq 140 - 150$$

$$\Gamma(T) \simeq T^4 e^{-\frac{S_3(T)}{T}}$$

$$S_3(T) = \int dr^3 \left\{ \frac{1}{2} \left(\vec{\nabla}\varphi \right)^2 + V_{\text{eff}}(\varphi, T) \right\}$$

Behavior of S_3/T↑

GWs from 1stOPT

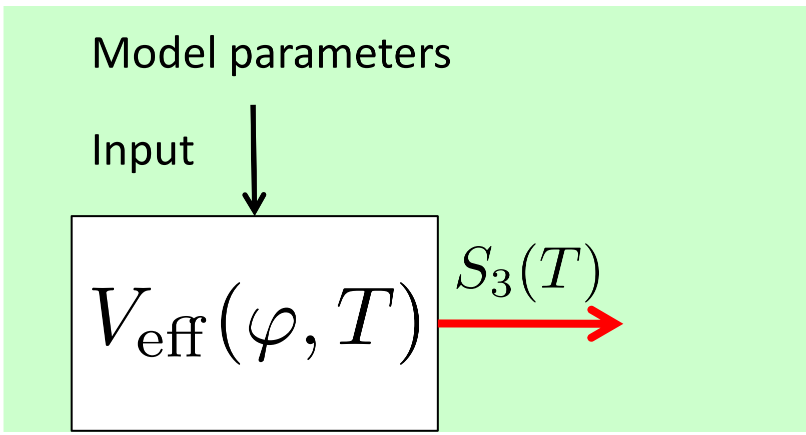

Definition of phase transition temperature T_t

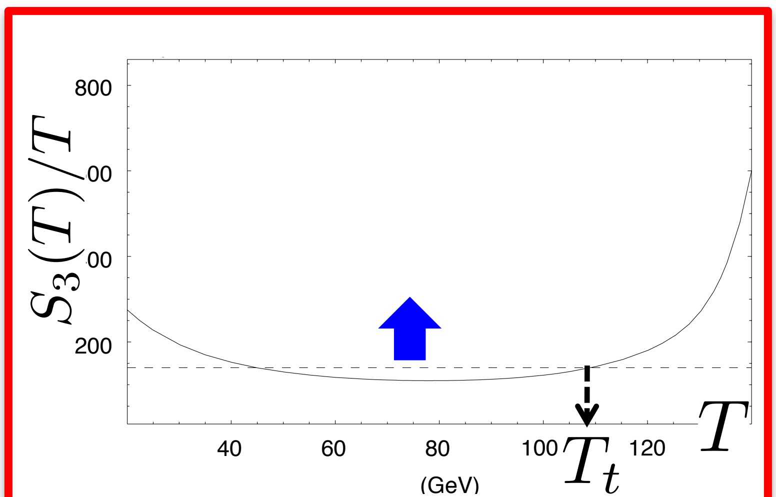

$$\boxed{\left.\frac{\Gamma}{H^4}\right|_{T=T_t} \simeq 1} \quad \leftrightarrows \quad \boxed{\left.\frac{S_3(T)}{T}\right|_{T=T_t} \simeq 140 - 150}$$

Model parameters are constrained.

R. Apreda et al., NPB**631**, 342 (2002)

Behavior of S_3/T↑

Phase transition - Characteristic parameters

Model parameters

Input ↓

$$V_{\rm eff}(\varphi, T) \longrightarrow \boxed{\alpha,\ \tilde{\beta}}_{\ @T=T_t}$$

- α is defined as $\alpha \equiv \left.\frac{\epsilon}{\rho_{\rm rad}}\right|_{T=T_t}$ is energy density of rad.)
  - Latent heat: $\epsilon(T) \equiv -\Delta V_{\rm eff}(\varphi_B(T), T) + T\frac{\partial \Delta V_{\rm eff}(\varphi_B(T))}{\partial T}$ cf. U=-F+T(dF/dT)

"Normalized difference of the potential minima"

- β is defined as $\beta \equiv \left.\frac{1}{\Gamma}\frac{d\Gamma}{dt}\right|_{t=t_t} \rightarrow$ $\tilde{\beta}\left(\equiv \frac{\beta}{H_t}\right) = T_t \left.\frac{d(S_3(T)/T)}{dT}\right|_{T=T_t}$

"~How fast the minimum goes down"

GWs from 1stOPT

C. Caprini *et al.*, JCAP**1604**, 001 (2016)

Expanding
bubbles of the broken phase

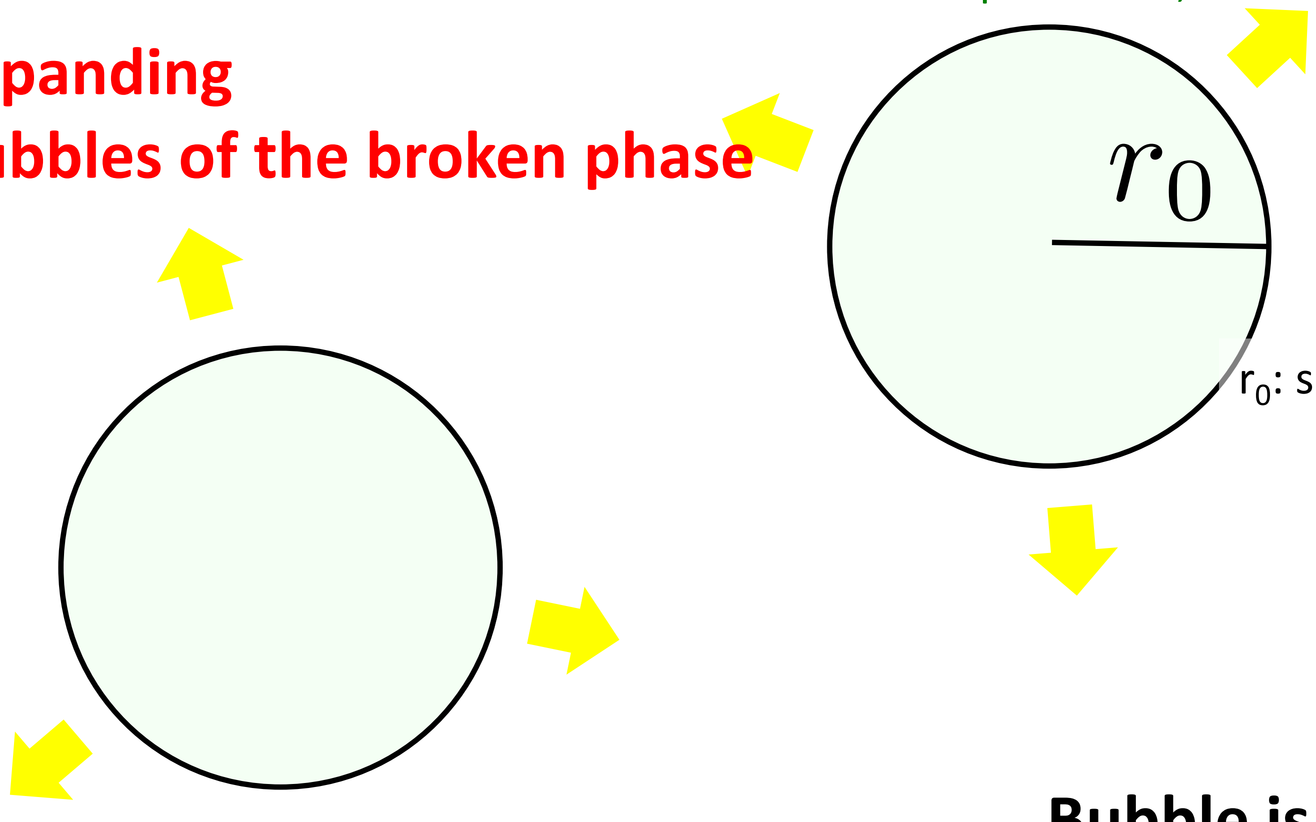

r_0: size of critical bubble

Bubble is spherical
No GW occurs

GWs from 1^{st}OPT

C. Caprini *et al.*, JCAP**1604**, 001 (2016)

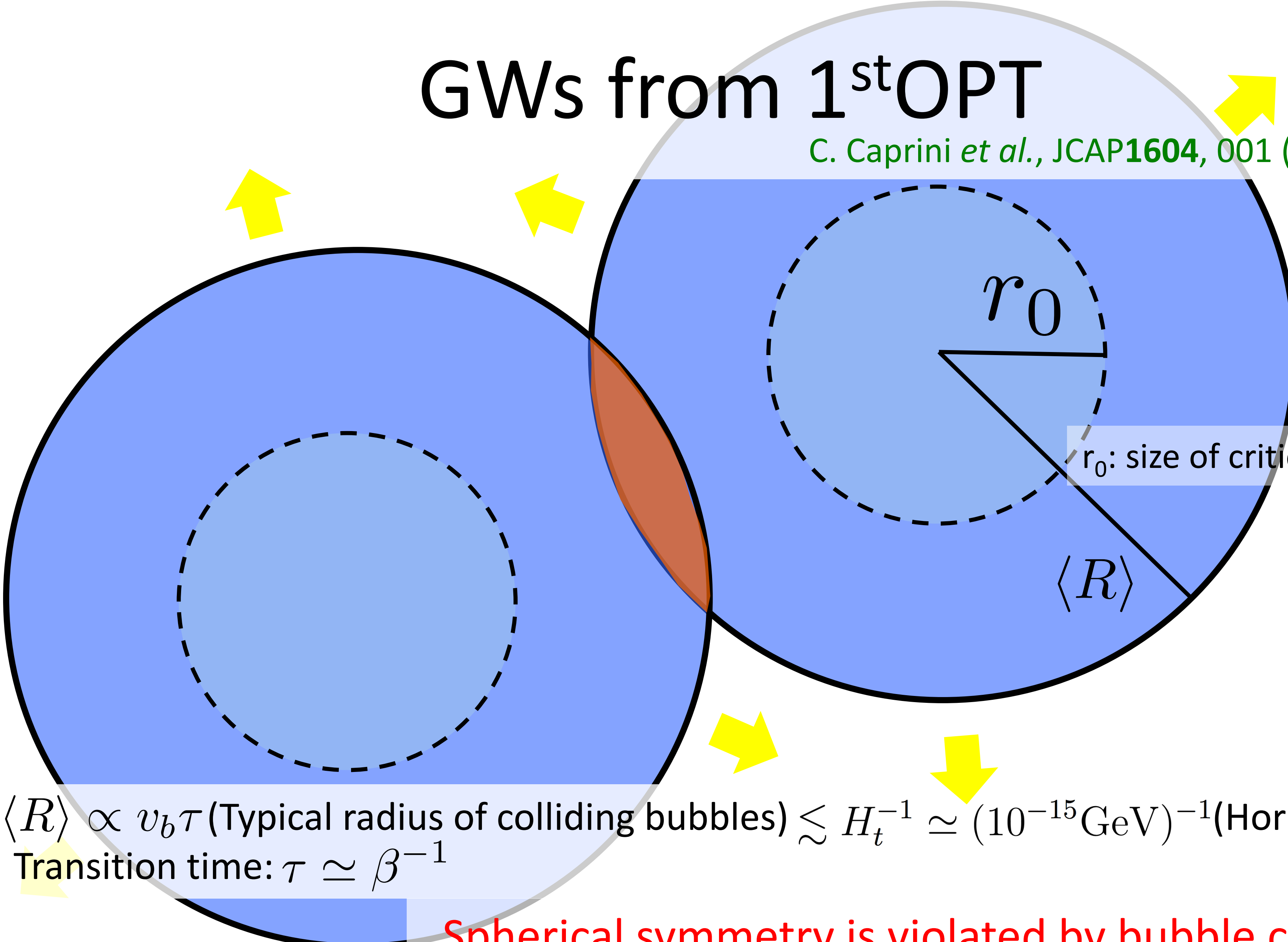

r_0: size of critical bubble

$\langle R \rangle \propto v_b \tau$ (Typical radius of colliding bubbles) $\lesssim H_t^{-1} \simeq (10^{-15}\mathrm{GeV})^{-1}$ (Horizon size),
Transition time: $\tau \simeq \beta^{-1}$

Spherical symmetry is violated by bubble collisions

GWs from 1stOPT

C. Caprini *et al.*, JCAP**1604**, 001 (2016)

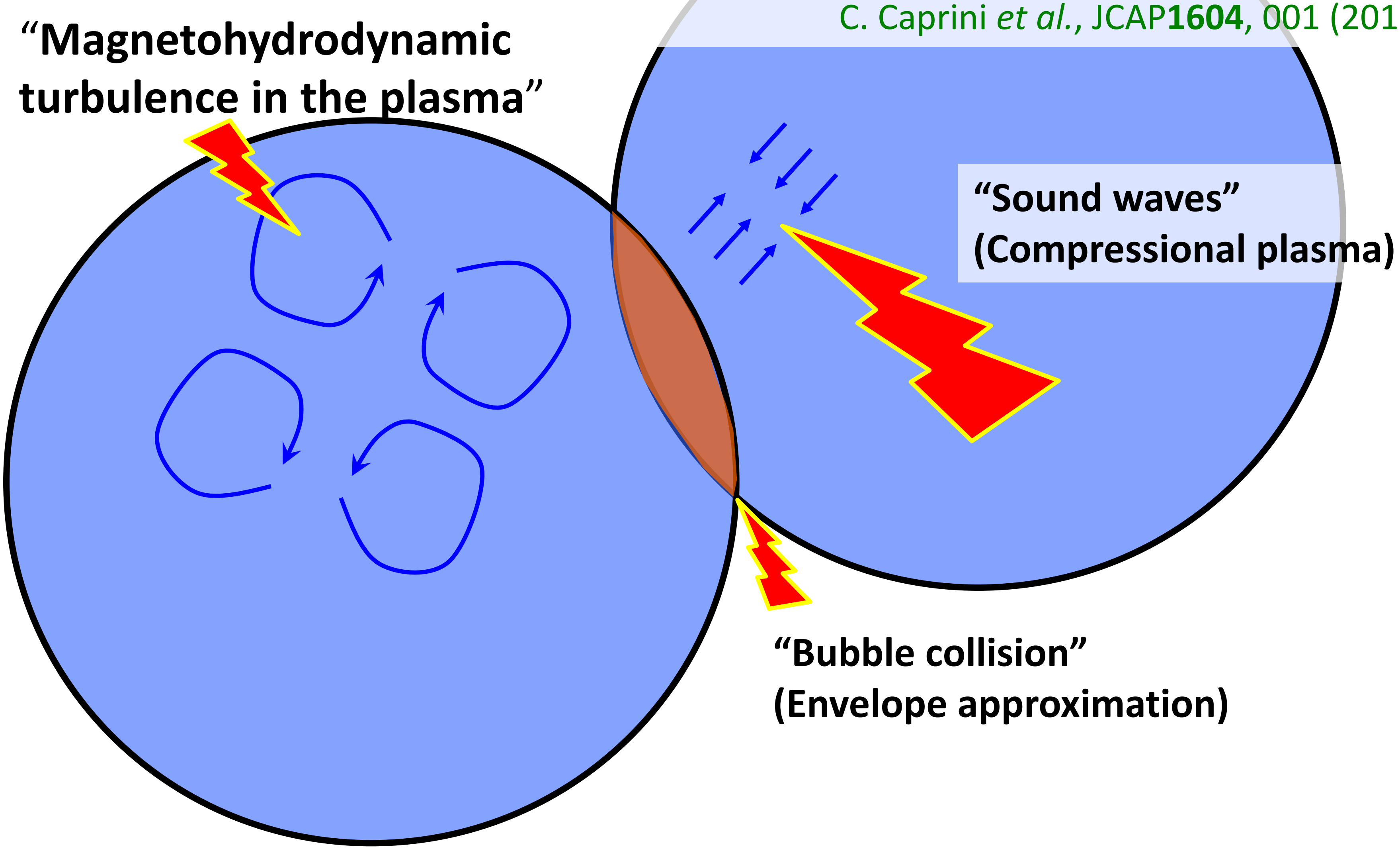

Relic abundance of GWs

(*) C. Caprini *et al.*, JCAP**1604**, 001 (2016)

Model parameters

Input

$V_{\rm eff}(\varphi, T)$ → $\alpha,\ \tilde{\beta}$ @T=T_t —Prediction*→ $\Omega_{\rm GW}(f)h^2$ (Observable)

Relic abundance of GWs @ peak frequency

$$\widetilde{\Omega}_{\rm sw}h^2 \simeq 2.65\times 10^{-6}\frac{v_b}{\tilde{\beta}}\left(\frac{\kappa(v_b,\alpha)\alpha}{1+\alpha}\right)^2 \quad @\ \tilde{f}_{\rm sw}\simeq 1.9\times 10^{-5}\ {\rm Hz}\frac{\tilde{\beta}(T_t/100\ {\rm GeV})}{v_b}$$

$$\widetilde{\Omega}_{\rm env}h^2 \simeq \frac{1.84\times 10^{-6}v_b^3}{(0.42+v_b^2)\tilde{\beta}^2}\left(\frac{\kappa(v_b,\alpha)\alpha}{1+\alpha}\right)^2 \quad @\ \tilde{f}_{\rm env}\simeq 1.0\times 10^{-5}\ {\rm Hz}\frac{\tilde{\beta}(T_t/100\ {\rm GeV})}{1.8-0.1v_b+v_b^2}$$

$$\widetilde{\Omega}_{\rm turb}h^2 \simeq \frac{9.35\times 10^{-8}v_b^2}{0.00354v_b\tilde{\beta}+\tilde{\beta}^2}\left(\frac{\epsilon\kappa(v_b,\alpha)\alpha}{1+\alpha}\right)^{3/2} \quad @\ \tilde{f}_{\rm turb}\simeq 2.7\times 10^{-5}\ {\rm Hz}\frac{\tilde{\beta}(T_t/100\ {\rm GeV})}{v_b}$$

Origins of GWs from EWPT

C. Caprini *et al.*, arXiv:1512.06239 [astro-ph.CO] (review)

2.1 Contributions to the Gravitational Wave Spectrum

To varying degrees, three processes are involved in the production of GWs at a first-order PT:

- Collisions of bubble walls and (where relevant) shocks in the plasma. This can be treated by a technique now generally referred to as the 'envelope approximation' [10–15]. As described below, this approximation can be used to compute the contribution to the GW spectrum from the scalar field, ϕ, itself.
- Sound waves in the plasma after the bubbles have collided but before expansion has dissipated the kinetic energy in the plasma [16–19].
- Magnetohydrodynamic (MHD) turbulence in the plasma forming after the bubbles have collided [20–25].

We improve our analysis in accordance with the recent simulation result.

Recent work of other souse of GW "sound wave"

M. Hindmarsh, *et al.*, PRL **112**, 041301 (2014); arXiv:1504.03291 [astro-ph.CO].

Numerical simulations of acoustically generated gravitational waves at a first order phase transition

Mark Hindmarsh,[1,2,*] Stephan J. Huber,[1,†] Kari Rummukainen,[2,‡] and David J. Weir[3,§]

[1] *Department of Physics and Astronomy, University of Sussex, Falmer, Brighton BN1 9QH, U.K.*
[2] *Department of Physics and Helsinki Institute of Physics, PL 64, FI-00014 University of Helsinki, Finland*
[3] *Institute of Mathematics and Natural Sciences, University of Stavanger, 4036 Stavanger, Norway*

(Dated: April 14, 2015)

We present details of numerical simulations of the gravitational radiation produced by a first order thermal phase transition in the early universe. We confirm that the dominant source of gravitational waves is sound waves generated by the expanding bubbles of the low-temperature phase. We demonstrate that the sound waves have a power spectrum with power-law form between the scales set by the average bubble separation (which sets the length scale of the fluid flow L_f) and the bubble wall width. The sound waves generate gravitational waves whose power spectrum also has a power-law form, at a rate proportional to L_f and the square of the fluid kinetic energy density. We identify a dimensionless parameter $\tilde{\Omega}_{GW}$ characterising the efficiency of this "acoustic" gravitational wave production whose value is $8\pi\tilde{\Omega}_{GW} \simeq 0.8 \pm 0.1$ across all our simulations. We compare the acoustic gravitational waves with the standard prediction from the envelope approximation. Not only is the power spectrum steeper (apart from an initial transient) but the gravitational wave energy density is generically two orders of magnitude or more larger.

Origins of GWs from EWPT

C. Caprini *et al.*, arXiv:1512.06239 [astro-ph.CO] (review)

- Vacuum bubble velocity v_b

- Efficiency factor $\kappa(v_b, \alpha)$

$$\widetilde{\Omega}_{\rm sw} h^2 \simeq 2.65 \times 10^{-6} \frac{v_b}{\tilde{\beta}} \left(\frac{\kappa(v_b,\alpha)\alpha}{1+\alpha} \right)^2 \quad @ \ \tilde{f}_{\rm sw} \simeq 1.9 \times 10^{-5} {\rm Hz} \frac{\tilde{\beta}}{v_b}$$

$$\widetilde{\Omega}_{\rm env} h^2 \simeq \frac{1.84 \times 10^{-6} v_b^3}{(0.42 + v_b^2)\tilde{\beta}^2} \left(\frac{\kappa(v_b,\alpha)\alpha}{1+\alpha} \right)^2 \quad @ \ \tilde{f}_{\rm env} \simeq 1.0 \times 10^{-5} {\rm Hz} \frac{\tilde{\beta}}{1.8 - 0.1 v_b + v_b^2}$$

$$\widetilde{\Omega}_{\rm turb} h^2 \simeq \frac{9.35 \times 10^{-8} v_b^2}{0.00354 v_b \tilde{\beta} + \tilde{\beta}^2} \left(\frac{\epsilon\kappa(v_b,\alpha)\alpha}{1+\alpha} \right)^{3/2} \quad @ \ \tilde{f}_{\rm turn} \simeq 2.7 \times 10^{-5} {\rm Hz} \frac{\tilde{\beta}}{v_b}$$

Origins of GWs from EWPT

C. Caprini *et al.*, arXiv:1512.06239 [astro-ph.CO] (review)

- Vacuum bubble velocity v_b

- Efficiency factor $\kappa(v_b, \alpha)$

$$\kappa(v_b, \alpha) \simeq O(0.01 - 0.1)$$

J.R.Espinosa, *et al*, JCAP **1006**, 028 (2010)

$$\widetilde{\Omega}_{\rm sw} h^2 \simeq 2.65 \times 10^{-6} \frac{v_b}{\tilde{\beta}} \left(\frac{\kappa(v_b, \alpha)\alpha}{1+\alpha} \right)^2 \quad @ \quad \tilde{f}_{\rm sw} \simeq 1.9 \times 10^{-5} {\rm Hz} \frac{\tilde{\beta}}{v_b}$$

$$\widetilde{\Omega}_{\rm env} h^2 \simeq \frac{1.84 \times 10^{-6} v_b^3}{(0.42 + v_b^2)\tilde{\beta}^2} \left(\frac{\kappa(v_b, \alpha)\alpha}{1+\alpha} \right)^2 \quad @ \quad \tilde{f}_{\rm env} \simeq 1.0 \times 10^{-5} {\rm Hz} \frac{\tilde{\beta}}{1.8 - 0.1 v_b + v_b^2}$$

$$\widetilde{\Omega}_{\rm turb} h^2 \simeq \frac{9.35 \times 10^{-8} v_b^2}{0.00354 v_b \tilde{\beta} + \tilde{\beta}^2} \left(\frac{\epsilon\kappa(v_b, \alpha)\alpha}{1+\alpha} \right)^{3/2} \quad @ \quad \tilde{f}_{\rm turn} \simeq 2.7 \times 10^{-5} {\rm Hz} \frac{\tilde{\beta}}{v_b}$$

Origins of GWs from EWPT

C. Caprini *et al.*, arXiv:1512.06239 [astro-ph.CO] (review)

- Vacuum bubble velocity v_b

- Efficiency factor $\kappa(v_b, \alpha)$

$$\kappa(v_b, \alpha) \simeq O(0.01 - 0.1)$$

J.R.Espinosa, *et al*, JCAP **1006**, 028 (2010)

- The fraction of bulk motion from the bubble walls

The result from resent simulation

$$\epsilon \simeq 0.05 - 0.10$$

Hindmarsh, Huber, Rummukainen, Weir, PRD **92**, no. 12, 123009 (2015)

$$\widetilde{\Omega}_{\rm sw} h^2 \simeq 2.65 \times 10^{-6} \frac{v_b}{\tilde{\beta}} \left(\frac{\kappa(v_b, \alpha)\alpha}{1+\alpha} \right)^2 \quad @ \quad \tilde{f}_{\rm sw} \simeq 1.9 \times 10^{-5} {\rm Hz} \frac{\tilde{\beta}}{v_b}$$

$$\widetilde{\Omega}_{\rm env} h^2 \simeq \frac{1.84 \times 10^{-6} v_b^3}{(0.42 + v_b^2)\tilde{\beta}^2} \left(\frac{\kappa(v_b, \alpha)\alpha}{1+\alpha} \right)^2 \quad @ \quad \tilde{f}_{\rm env} \simeq 1.0 \times 10^{-5} {\rm Hz} \frac{\tilde{\beta}}{1.8 - 0.1 v_b + v_b^2}$$

$$\widetilde{\Omega}_{\rm turb} h^2 \simeq \frac{9.35 \times 10^{-8} v_b^2}{0.00354 v_b \tilde{\beta} + \tilde{\beta}^2} \left(\frac{\epsilon\kappa(v_b, \alpha)\alpha}{1+\alpha} \right)^{3/2} \quad @ \quad \tilde{f}_{\rm turn} \simeq 2.7 \times 10^{-5} {\rm Hz} \frac{\tilde{\beta}}{v_b}$$

$(\alpha, \tilde{\beta}) \Leftrightarrow (f, \Omega_{GW}h^2)_{new}$

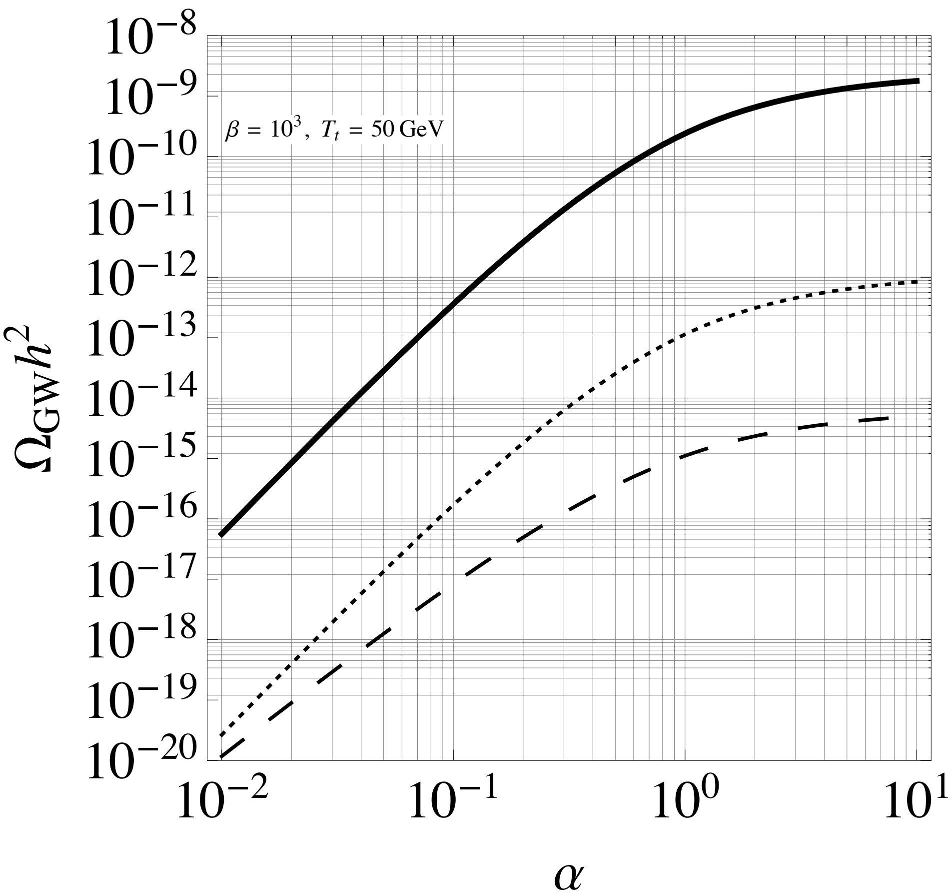

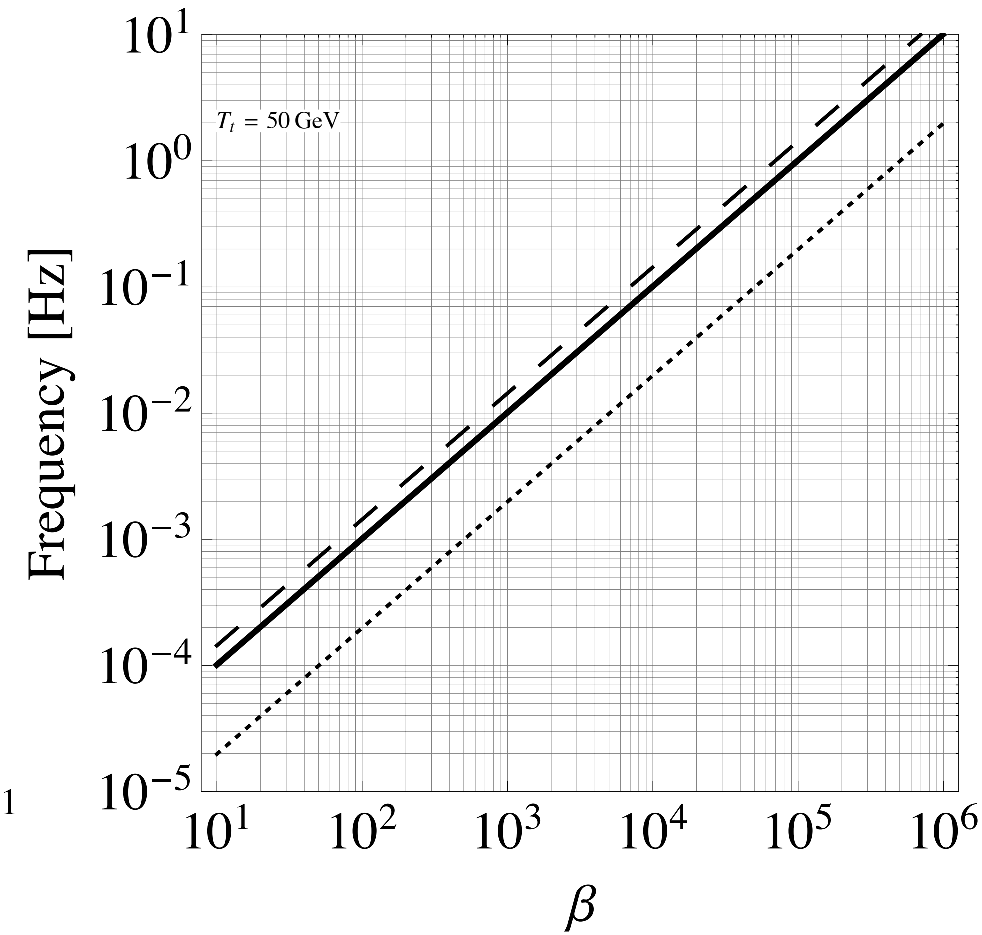

(α, βtilde)_exp. by New spectra (T_t=50GeV)

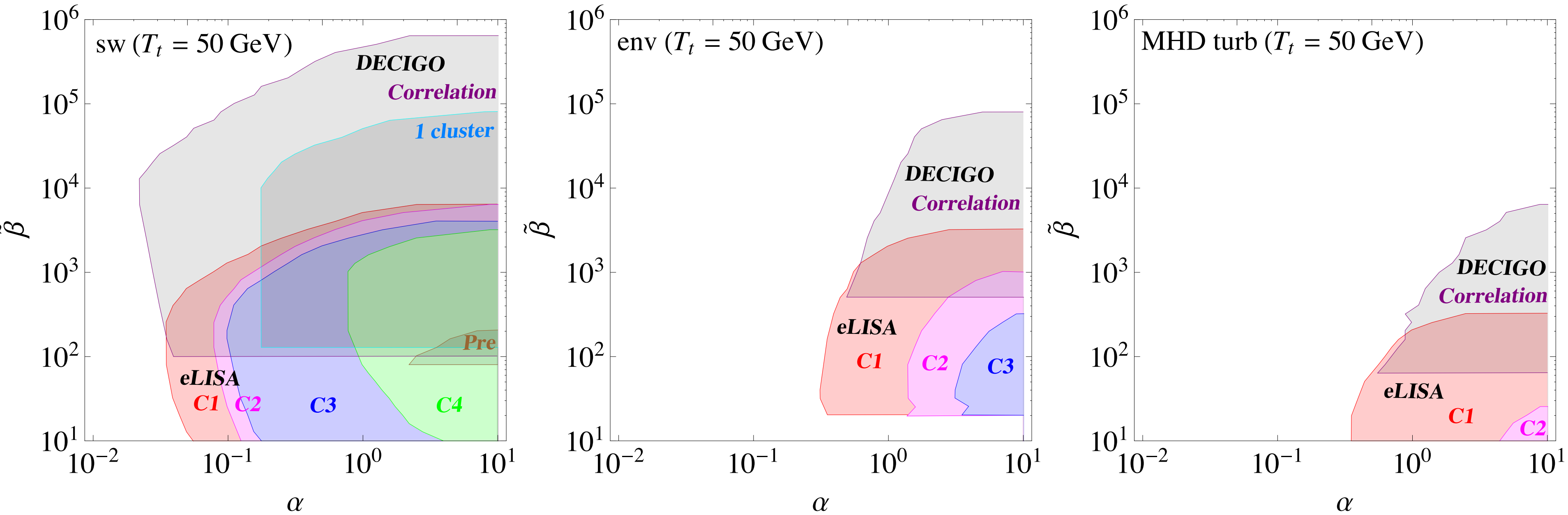

(α, βtilde)_exp. by New spectra (T_t=100GeV)

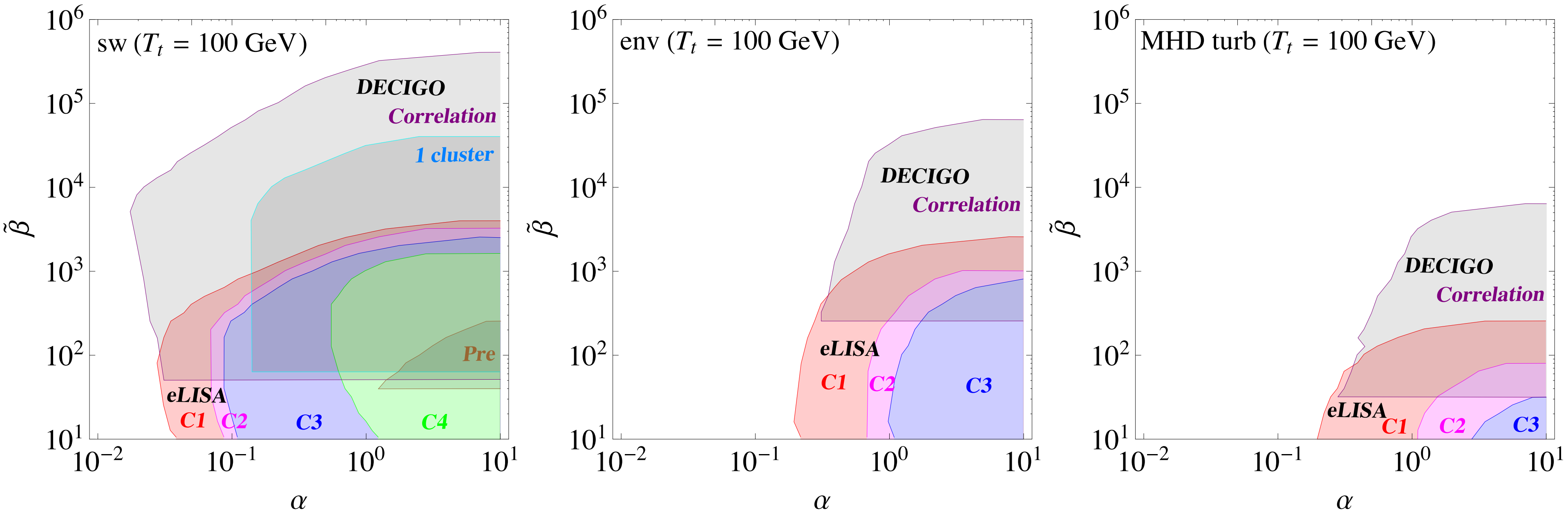

Efficiency factor κ(v_b , α)

J. R. Espinosa, *et al*, JCAP **1006**, 028 (2010)

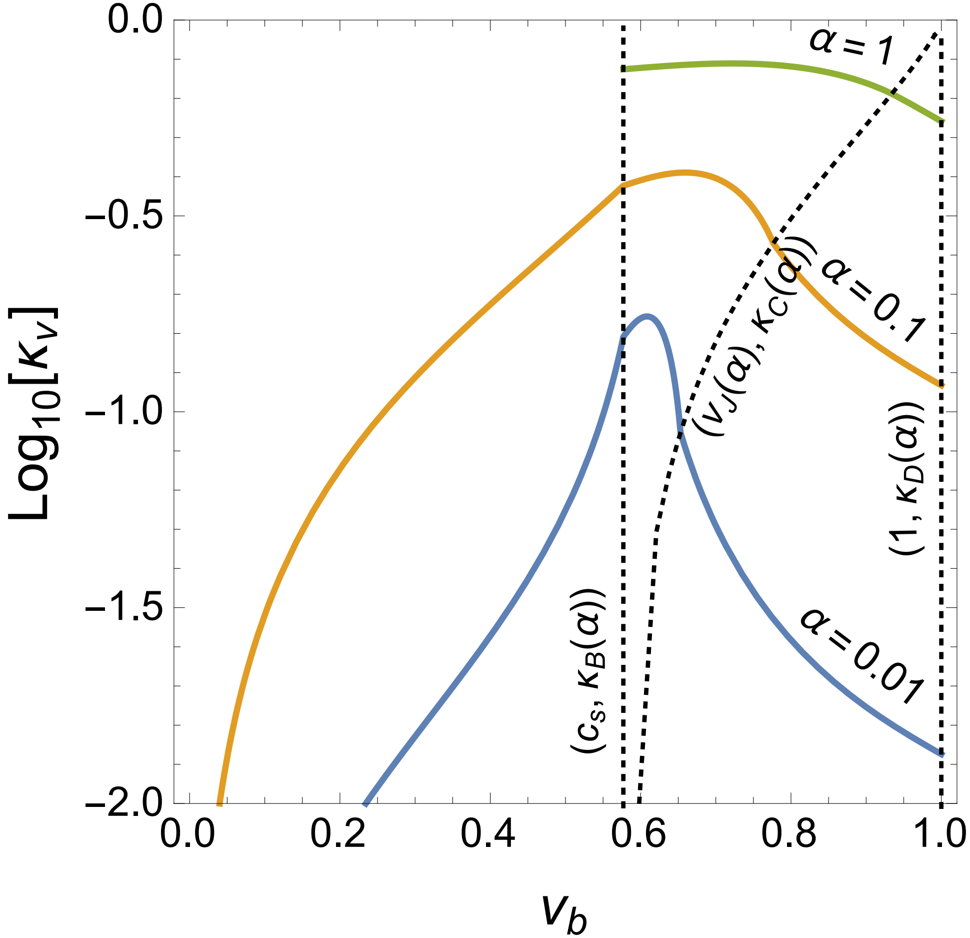

A Numerical fits to the efficiency coefficients

J. R. Espinosa, *et al.*

In this section we provide fits to the numerical results of section 4. These fits facilitate the functions $\kappa(\xi_w, \alpha_N)$ and $\alpha_+(\xi_w, \alpha_N)$ without solving the flow equations and with a precision better that 15% in the region $10^{-3} < \alpha_N < 10$.

In order to fit the function $\kappa(\xi_w, \alpha_N)$, we split the parameter space into three regions and provide approximations for the four boundary cases and three families of functions that interpolate in-between: For small wall velocities one obtains ($\xi_w \ll c_s$)

$$\kappa_A \simeq \xi_w^{6/5} \frac{6.9\alpha_N}{1.36 - 0.037\sqrt{\alpha_N} + \alpha_N} . \tag{A.1}$$

For the transition from subsonic to supersonic deflagrations ($\xi_w = c_s$)

$$\kappa_B \simeq \frac{\alpha_N^{2/5}}{0.017 + (0.997 + \alpha_N)^{2/5}} . \tag{A.2}$$

ξ_J is same as our $v_b(\alpha)$

For Jouguet detonations ($\xi_w = \xi_J$), as stated in eq. (4.2)

$$\kappa_C \simeq \frac{\sqrt{\alpha_N}}{0.135 + \sqrt{0.98 + \alpha_N}} \quad \text{and} \quad \xi_J = \frac{\sqrt{\frac{2}{3}\alpha_N + \alpha_N^2} + \sqrt{1/3}}{1 + \alpha_N} . \tag{A.3}$$

And finally for very large wall velocity, ($\xi_w \to 1$) as stated in eq. (4.4)

$$\kappa_D \simeq \frac{\alpha_N}{0.73 + 0.083\sqrt{\alpha_N} + \alpha_N} . \tag{A.4}$$

For subsonic deflagrations a good fit to the numerical results is provided by

$$\boxed{\kappa(\xi_w \lesssim c_s) \simeq \frac{c_s^{11/5}\kappa_A\kappa_B}{(c_s^{11/5} - \xi_w^{11/5})\kappa_B + \xi_w c_s^{6/5}\kappa_A}} , \tag{A.5}$$

and for detonations by

$$\boxed{\kappa(\xi_w \gtrsim \xi_J) \simeq \frac{(\xi_J - 1)^3 \xi_J^{5/2}\xi_w^{-5/2}\kappa_C\kappa_D}{[(\xi_J - 1)^3 - (\xi_w - 1)^3]\xi_J^{5/2}\kappa_C + (\xi_w - 1)^3\kappa_D}} . \tag{A.6}$$

The numerical result for the hybrid (supersonic deflagration) region is well described by a cubic polynomial. As boundary conditions, one best uses the two values of κ and the first derivative of κ at $\xi_w = c_s$. Notice that the derivative of κ in ξ_w is not continuous at the point ξ_J. The derivative at $\xi_w = c_s$ is approximately given by

$$\delta\kappa \simeq -0.9 \log \frac{\sqrt{\alpha_N}}{1 + \sqrt{\alpha_N}} . \tag{A.7}$$

This differs from the derivative one would obtain from the fit in the region $\xi_w < c_s$, but mostly for values $\alpha \gtrsim 1$, where no solutions exist for $\xi_w < c_s$. The expression for supersonic deflagrations then reads

$$\boxed{\kappa(c_s < \xi_w < \xi_J) \simeq \kappa_B + (\xi_w - c_s)\delta\kappa + \frac{(\xi_w - c_s)^3}{(\xi_J - c_s)^3}[\kappa_C - \kappa_B - (\xi_J - c_s)\delta\kappa]} . \tag{A.8}$$

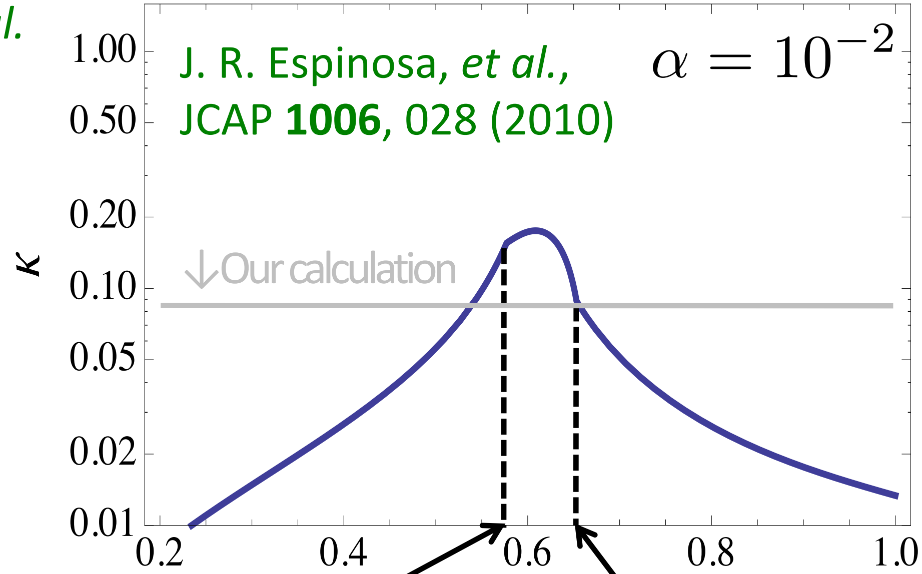

$c_s = 0.577$ ξ_w $\boxed{\xi_J(\alpha)}$

$$\tilde{\Omega}_{\rm coll}h^2 \simeq \frac{1.8 \times 10^{-6}(\kappa(\alpha, \xi_w))^2\xi_w^3}{0.42 + \xi_w^2} \times \left(\frac{\alpha}{1+\alpha}\right)^2 \tilde{\beta}^{-2}$$

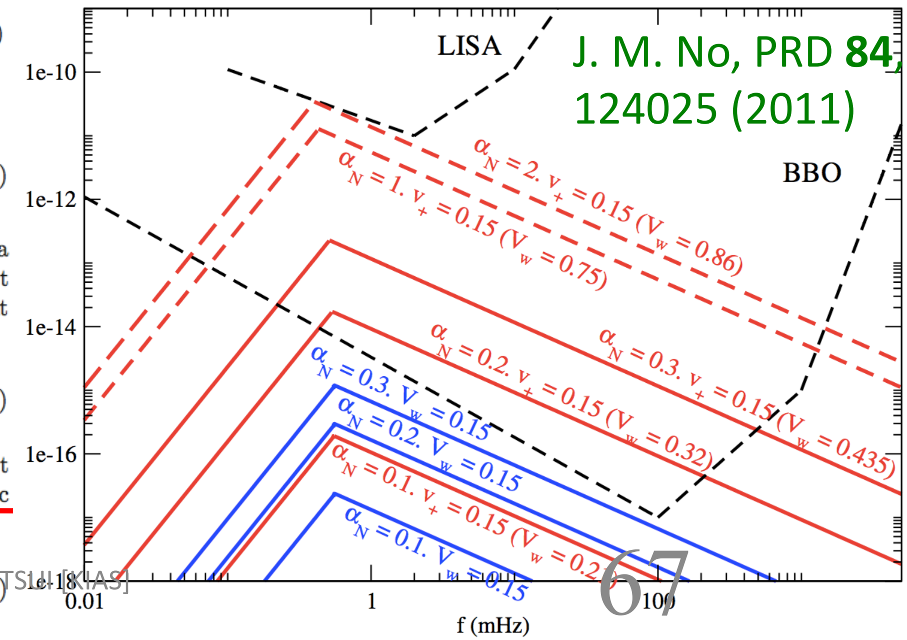

Contour plot of α on (ξ_w, v_+) plane

α is given by effective potential.

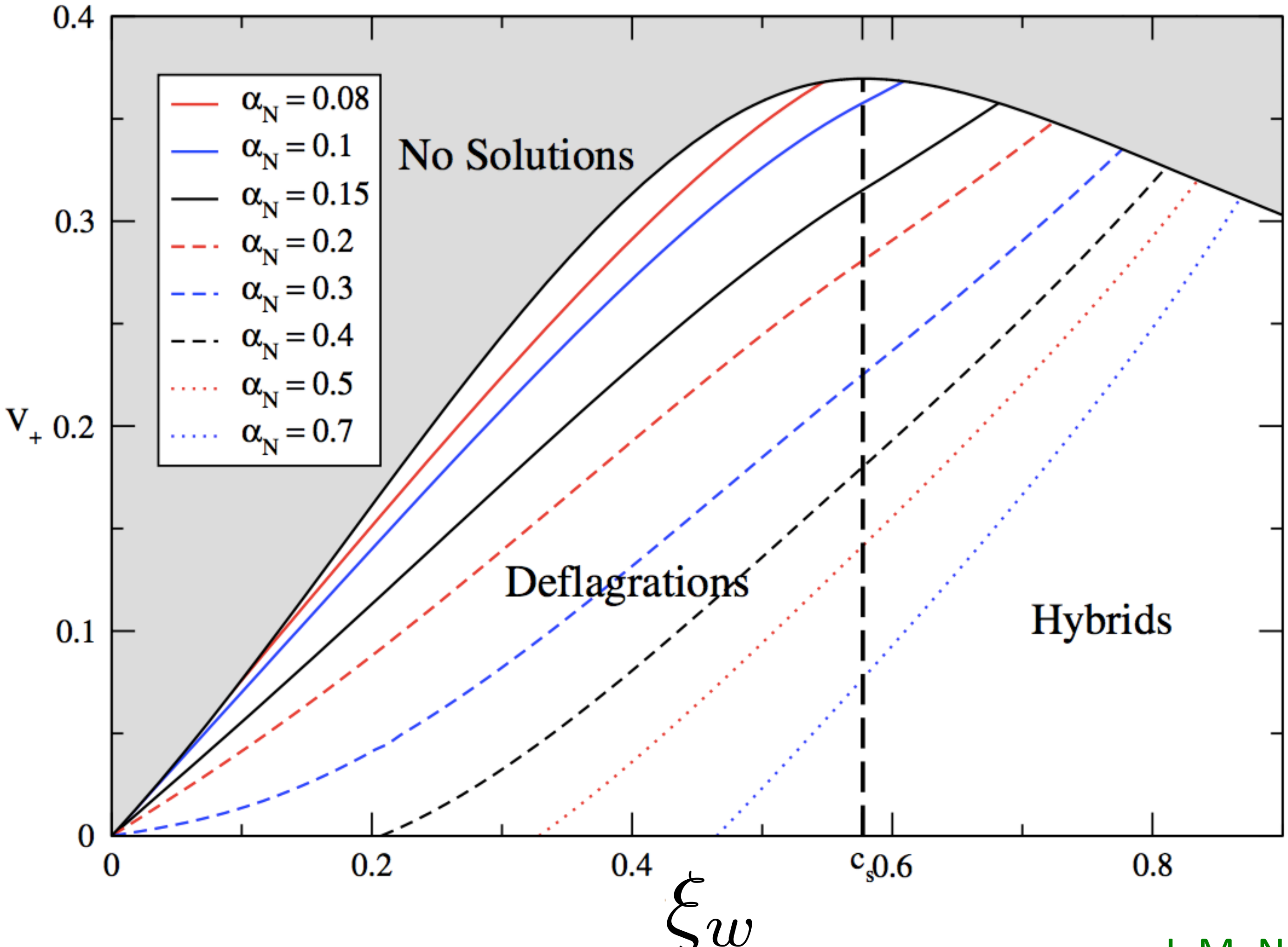

Diffusion upper bound of EWBG

EWBG requires small ξ_w
⇆GW requires large

J. M. No, PRD84, 124025 (2011)

Contour plot of v_+ on (ξ_w, α) plane

α is given by effective potential.

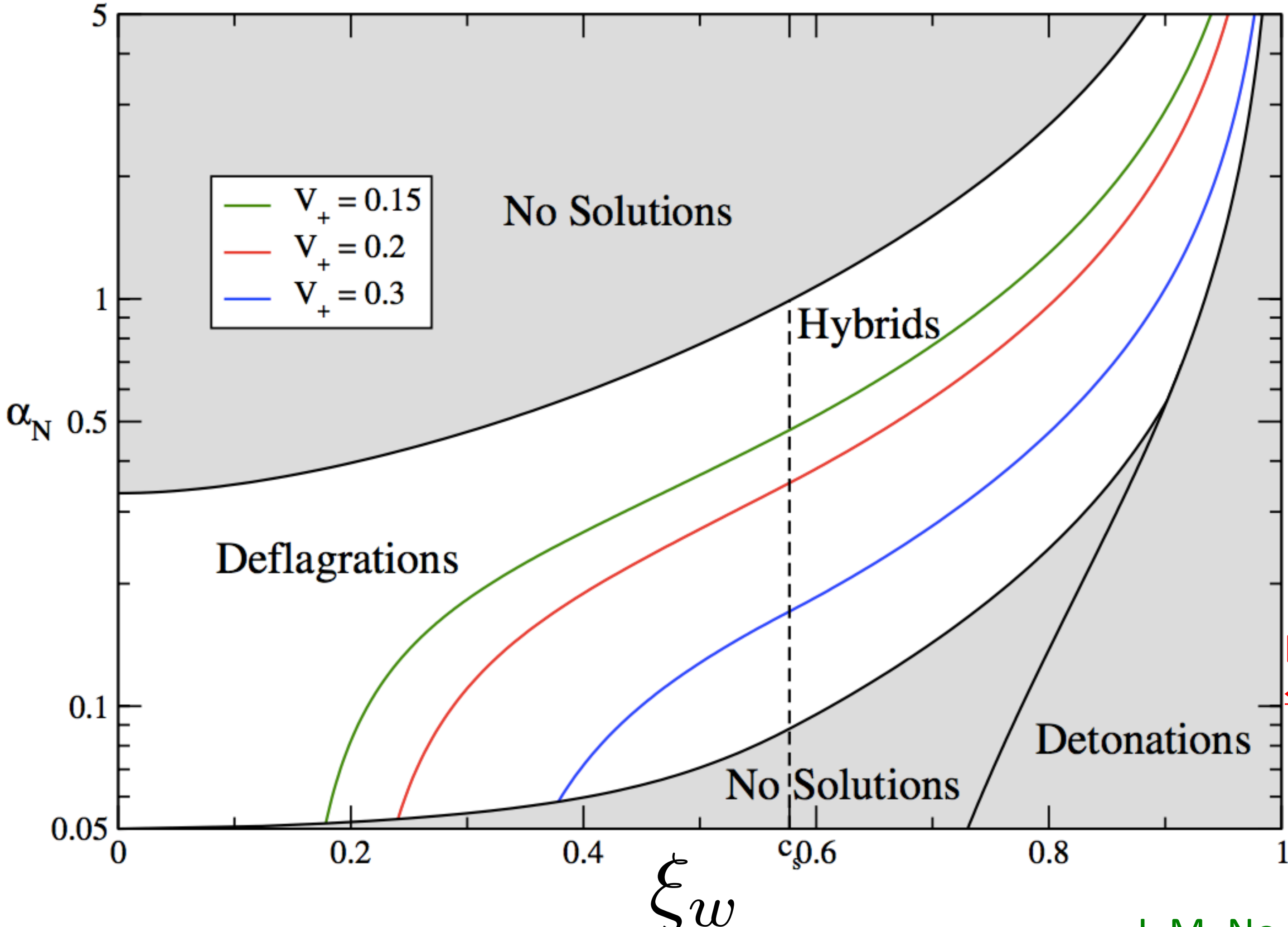

EWBG requires small ξ_w

⇆GW requires large

J. M. No, PRD84, 124025 (2011)